12th International Conference
on Elastic and Diffractive Scattering
Forward Physics and QCD
May 21–25, 2007, DESY, Hamburg, Germany

Angular decorrelations in Mueller–Navelet jets and DIS

Agustín Sabio Vera (CERN)

In collaboration with
Florian Schwennsen (Hamburg U.)

NPB 746 (2006), hep–ph/0611151
NPB ??? (2007), hep–ph/ 0702158

$$\frac{d\hat{\sigma}}{d^2\vec{q}_1 d^2\vec{q}_2} = \frac{\pi^2 \bar{\alpha}_s^2}{2} \frac{f\left(\vec{q}_1, \vec{q}_2, \mathrm{Y}\right)}{q_1^2 q_2^2},$$

The gluon Green's function

$$f\left(\vec{q}_1, \vec{q}_2, \mathrm{Y}\right) = \int \frac{d\omega}{2\pi i} e^{\omega \mathrm{Y}} f_\omega\left(\vec{q}_1, \vec{q}_2\right),$$

carries the full dependence on Y and fulfills the NLO BFKL equation which, in the transverse momenta operator representation

$$\hat{q}\left|\vec{q}_i\right\rangle = \vec{q}_i\left|\vec{q}_i\right\rangle,$$

with normalization

$$\left\langle\vec{q}_1\right|\hat{1}\left|\vec{q}_2\right\rangle = \delta^{(2)}\left(\vec{q}_1 - \vec{q}_2\right),$$

can be written as

$$\left(\omega - \bar{\alpha}_s \hat{K}_0 - \bar{\alpha}_s^2 \hat{K}_1\right) \hat{f}_\omega = \hat{1}.$$

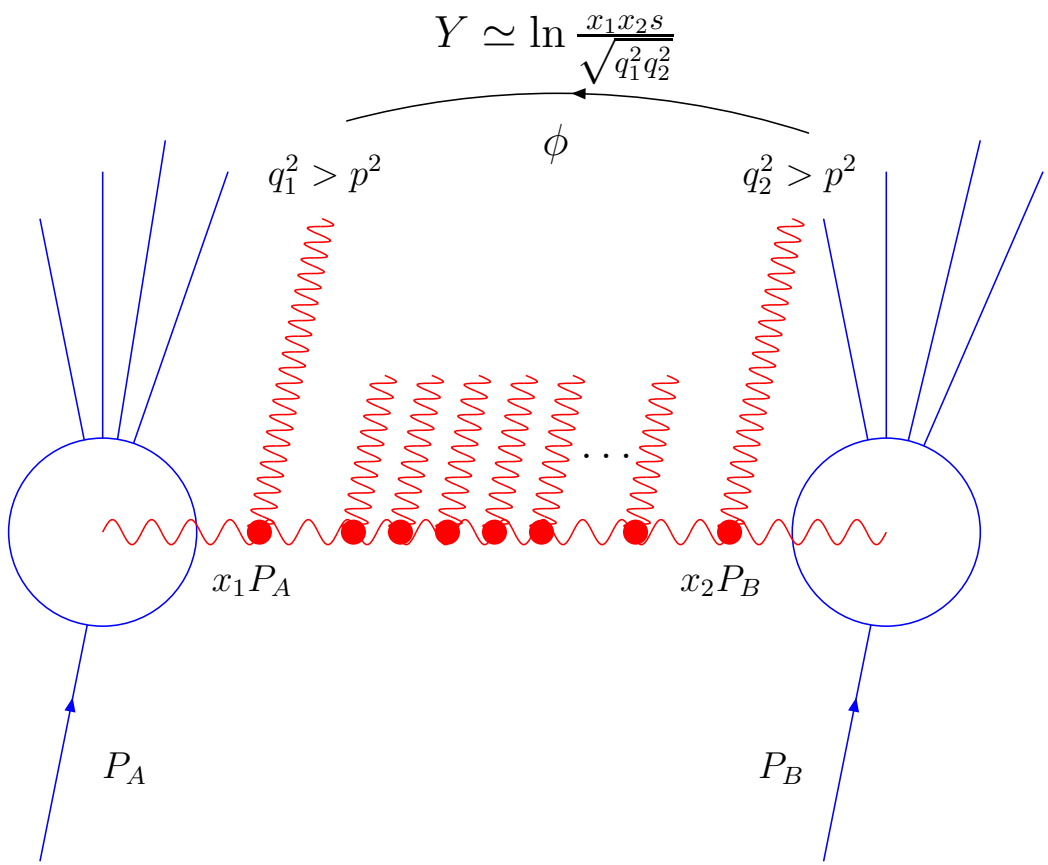

Figure 1: Representation of Mueller–Navelet jets at a hadron collider.

This representation is useful when it acts on the basis

$$\langle \vec{q}| \, \nu, n \rangle \quad = \quad \frac{1}{\pi\sqrt{2}} \left(q^2\right)^{i\nu - \frac{1}{2}} \, e^{in\theta},$$

As Y increases the azimuthal angle dependence is driven by the kernel. This is why we uses of the LO jet vertices which are much simpler than the NLO. We can write the differential cross section in the azimuthal angle $\phi = \theta_1 - \theta_2 - \pi$, where θ_i are the angles of the two tagged jets, as

$$\frac{d\hat{\sigma}\left(\alpha_s, \mathrm{Y}, p_{1,2}^2\right)}{d\phi} \quad = \quad \frac{\pi^2 \bar{\alpha}_s^2}{4\sqrt{p_1^2 p_2^2}} \sum_{n=-\infty}^{\infty} e^{in\phi} \, \mathcal{C}_n\left(\mathrm{Y}\right),$$

with

$$\mathcal{C}_n\left(\mathrm{Y}\right) \quad = \quad \frac{1}{2\pi} \int_{-\infty}^{\infty} \frac{d\nu}{\left(\frac{1}{4} + \nu^2\right)} \left(\frac{p_1^2}{p_2^2}\right)^{i\nu} e^{\chi\left(|n|, \frac{1}{2} + i\nu, \bar{\alpha}_s(p_1 p_2)\right)\mathrm{Y}},$$

and

$$\chi\left(n, \gamma, \bar{\alpha}_s\right) \quad \equiv \quad \bar{\alpha}_s \chi_0\left(n, \gamma\right) + \bar{\alpha}_s^2 \left(\chi_1\left(n, \gamma\right) - \frac{\beta_0}{8N_c} \frac{\chi_0\left(n, \gamma\right)}{\gamma\left(1 - \gamma\right)}\right).$$

$\mathcal{C}_n$ are not evaluated at the saddle point, but obtained by a numerical integration over the full range of ν. The LO kernel, $\hat{K}_0$, has eigenvalue

$$\chi_0(n,\gamma) = 2\psi(1) - \psi\left(\gamma + \frac{n}{2}\right) - \psi\left(1 - \gamma + \frac{n}{2}\right),$$

The eigenvalue of the scale invariant sector of the NLO kernel, $\hat{K}_1$, in the $\overline{\text{MS}}$–scheme, is

$$\begin{aligned}
\chi_1(n,\gamma) &= \mathcal{S}\chi_0(n,\gamma) + \frac{3}{2}\zeta(3) - \frac{\beta_0}{8N_c}\chi_0^2(n,\gamma) \\
&+ \frac{1}{4}\left[\psi''\left(\gamma + \frac{n}{2}\right) + \psi''\left(1 - \gamma + \frac{n}{2}\right) - 2\,\phi(n,\gamma) - 2\,\phi(n,1-\gamma)\right] \\
&- \frac{\pi^2\cos(\pi\gamma)}{4\sin^2(\pi\gamma)(1-2\gamma)}\left\{\left[3 + \left(1 + \frac{n_f}{N_c^3}\right)\frac{2 + 3\gamma(1-\gamma)}{(3-2\gamma)(1+2\gamma)}\right]\delta_n^0\right. \\
&\left. - \left(1 + \frac{n_f}{N_c^3}\right)\frac{\gamma(1-\gamma)}{2(3-2\gamma)(1+2\gamma)}\delta_n^2\right\},
\end{aligned}$$

where $\mathcal{S} = \left(4 - \pi^2 + 5\beta_0/N_c\right)/12$.

$$\begin{aligned}\phi(n,\gamma) &= \sum_{k=0}^{\infty} \frac{(-1)^{(k+1)}}{k+\gamma+\frac{n}{2}} \Big(\psi'(k+n+1) - \psi'(k+1) \\ &+(-1)^{(k+1)} \left(\beta'(k+n+1) + \beta'(k+1)\right) + \frac{\psi(k+1) - \psi(k+n+1)}{k+\gamma+\frac{n}{2}} \Big),\end{aligned}$$

with

$$4\,\beta'(\gamma) = \psi'\left(\frac{1+\gamma}{2}\right) - \psi'\left(\frac{\gamma}{2}\right).$$

The full cross section corresponds to the integration over the azimuthal angle. It only depends on the $n = 0$ component:

$$\hat{\sigma}\left(\alpha_s, \mathrm{Y}, p_{1,2}^2\right) = \frac{\pi^3 \bar{\alpha}_s^2}{2\sqrt{p_1^2 p_2^2}} \mathcal{C}_0\left(\mathrm{Y}\right).$$

We are interested in distributions sensitive to higher conformal spins. The average of the cosine of the azimuthal angle times an integer projects out the contribution from each of these angular components:

$$\langle \cos\left(m\phi\right) \rangle = \frac{\mathcal{C}_m\left(\mathrm{Y}\right)}{\mathcal{C}_0\left(\mathrm{Y}\right)}.$$

The associated ratios

$$\frac{\langle \cos\left(m\phi\right) \rangle}{\langle \cos\left(n\phi\right) \rangle} = \frac{\mathcal{C}_m\left(\mathrm{Y}\right)}{\mathcal{C}_n\left(\mathrm{Y}\right)}$$

can be used to remove the uncertainty associated to the $n = 0$ hard pomeron

intercept. All angular components together:

$$\frac{1}{\hat{\sigma}}\frac{d\hat{\sigma}}{d\phi} = \frac{1}{2\pi}\sum_{n=-\infty}^{\infty} e^{in\phi}\frac{\mathcal{C}_n\left(\mathrm{Y}\right)}{\mathcal{C}_0\left(\mathrm{Y}\right)} = \frac{1}{2\pi}\left\{1+2\sum_{n=1}^{\infty}\cos\left(n\phi\right)\left\langle\cos\left(n\phi\right)\right\rangle\right\}.$$

The BFKL resummation presents an instability at NLO. Our cross sections are very dependent on the renormalization scheme. The term proportional to χ_0 in χ_1 can be removed:

$$\Lambda_{\overline{\mathrm{MS}}} \to \Lambda_{\mathrm{GB}} = \Lambda_{\overline{\mathrm{MS}}} e^{\frac{2N_c}{\beta_0}\mathcal{S}}.$$

This is the gluon–bremsstrahlung (GB) scheme where some distributions become unphysical due to poor convergence of the series.

Convergence can be improved demanding compatibility with renormalization group evolution to all orders in the DIS limit, introducing a shift in anomalous dimension. So far these types of resummations have been performed for a BFKL kernel averaged over the azimuthal angle and only affect the zero conformal spin. We study the convergence of the eigenvalues for all angular components.

First we extract the poles at $\gamma = -\frac{n}{2}, 1+\frac{n}{2}$:

$$
\begin{aligned}
\chi_0(n,\gamma) &\simeq \frac{1}{\gamma+\frac{n}{2}} + \{\gamma \to 1-\gamma\}, \\
\chi_1(n,\gamma) &\simeq \frac{a_n}{\gamma+\frac{n}{2}} + \frac{b_n}{\left(\gamma+\frac{n}{2}\right)^2} - \frac{1}{2\left(\gamma+\frac{n}{2}\right)^3} + \frac{c\,\delta_n^2}{\gamma} + \{\gamma \to 1-\gamma\} \\
a_n &= \mathcal{S} - \frac{\pi^2}{24} + \frac{\beta_0}{4N_c}\mathrm{H}_n + \frac{1}{8}\left(\psi'\left(\frac{n+1}{2}\right) - \psi'\left(\frac{n+2}{2}\right)\right) \\
&+ \frac{1}{2}\psi'(n+1) \\
&- \frac{\delta_n^0}{36}\left(67 + 13\frac{n_f}{N_c^3}\right) - \frac{47\delta_n^2}{1800}\left(1+\frac{n_f}{N_c^3}\right), \\
-b_n &= \frac{\beta_0}{8N_c} + \frac{1}{2}\mathrm{H}_n + \frac{\delta_n^0}{12}\left(11 + 2\frac{n_f}{N_c^3}\right) + \frac{\delta_n^2}{60}\left(1+\frac{n_f}{N_c^3}\right), \\
c &= \frac{1}{24}\left(1+\frac{n_f}{N_c^3}\right).
\end{aligned}
$$

$\mathrm{H}_n = \psi(n+1) - \psi(1).$

We use the resumation scheme:

$$
\begin{aligned}
\omega \quad = \quad & \bar{\alpha}_s \left(1 + \mathcal{A}_n \bar{\alpha}_s\right) \left\{ 2\,\psi(1) - \psi\left(\gamma + \frac{|n|}{2} + \frac{\omega}{2} + \mathcal{B}_n \bar{\alpha}_s\right) \right. \\
& \left. - \psi\left(1 - \gamma + \frac{|n|}{2} + \frac{\omega}{2} + \mathcal{B}_n \bar{\alpha}_s\right) \right\} \\
& + \bar{\alpha}_s^2 \left\{ \chi_1(|n|, \gamma) - \frac{\beta_0}{8N_c} \frac{\chi_0(n,\gamma)}{\gamma(1-\gamma)} - \mathcal{A}_n \chi_0(|n|, \gamma) \right) \\
& + \left(\psi'\left(\gamma + \frac{|n|}{2}\right) + \psi'\left(1 - \gamma + \frac{|n|}{2}\right) \right) \left(\frac{\chi_0(|n|, \gamma)}{2} + \mathcal{B}_n \right) \Bigg\},
\end{aligned}
$$

$$
\begin{aligned}
\mathcal{A}_n \quad &= \quad a_n + \psi'(n+1), \\
\mathcal{B}_n \quad &= \quad \frac{1}{2}\mathrm{H}_n - b_n
\end{aligned}
$$

The solution is very well approximated to "All–poles" by

$$\omega = \bar{\alpha}_s \chi_0 \left(|n|, \gamma\right) + \bar{\alpha}_s^2 \left(\chi_1 \left(|n|, \gamma\right) - \frac{\beta_0}{8N_c} \frac{\chi_0 \left(n, \gamma\right)}{\gamma \left(1-\gamma\right)} \right)$$

$$+ \left\{ \sum_{m=0}^{\infty} \left[-m + b_n \, \bar{\alpha}_s - \frac{|n|}{2} - \gamma + \sqrt{2 \left(\bar{\alpha}_s + a_n \, \bar{\alpha}_s^2\right) + \left(m - b_n \, \bar{\alpha}_s + \gamma + \frac{|n|}{2} \right)^2} \right.\right.$$

$$\left.\left. - \left(\frac{\bar{\alpha}_s + a_n \bar{\alpha}_s^2}{\gamma + m + \frac{|n|}{2}} + \frac{\bar{\alpha}_s^2 \, b_n}{\left(\gamma + m + \frac{|n|}{2}\right)^2} - \frac{\bar{\alpha}_s^2}{2 \left(\gamma + m + \frac{|n|}{2}\right)^3} \right) \right] + \left\{ \gamma \to 1 - \gamma \right\} \right\}$$

$$\omega = \alpha \left(2\psi(1) - \psi\left(\gamma + \frac{\omega}{2}\right) - \psi\left(1 - \gamma + \frac{\omega}{2}\right) \right)$$

$$\omega = \int_0^1 \frac{dx}{1-x} \left(\left(x^{\gamma-1} + x^{-\gamma}\right) \sqrt{\frac{2\alpha}{\log^2 x}} J_1 \left(\sqrt{2\alpha \log^2 x} \right) - 2\alpha \right)$$

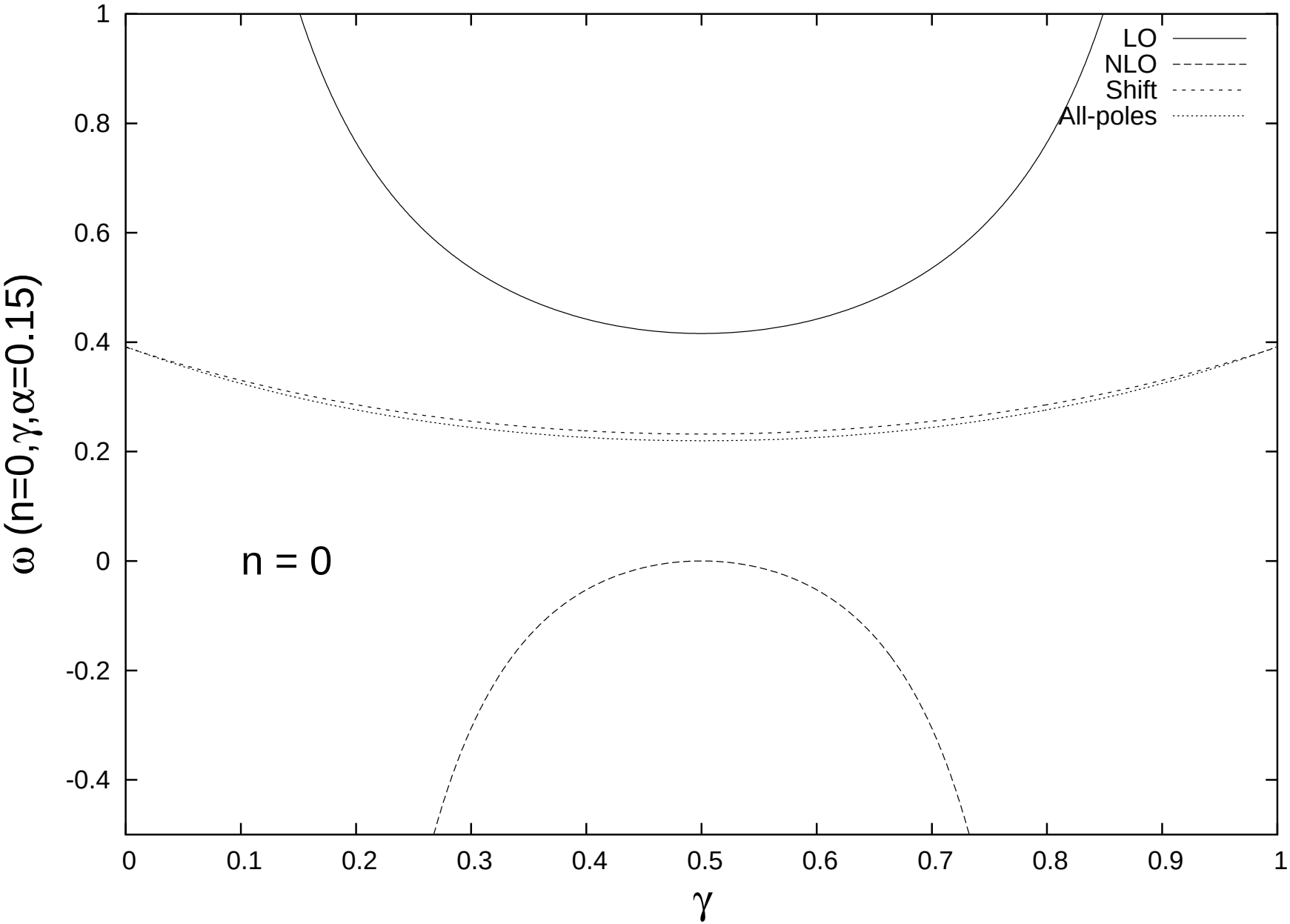
LO
NLO
Shift
All-poles
n = 0
ω (n=0,γ,α=0.15)
γ
1
0.8
0.6
0.4
0.2
0
-0.2
-0.4
0
0.1
0.2
0.3
0.4
0.5
0.6
0.7
0.8
0.9
1

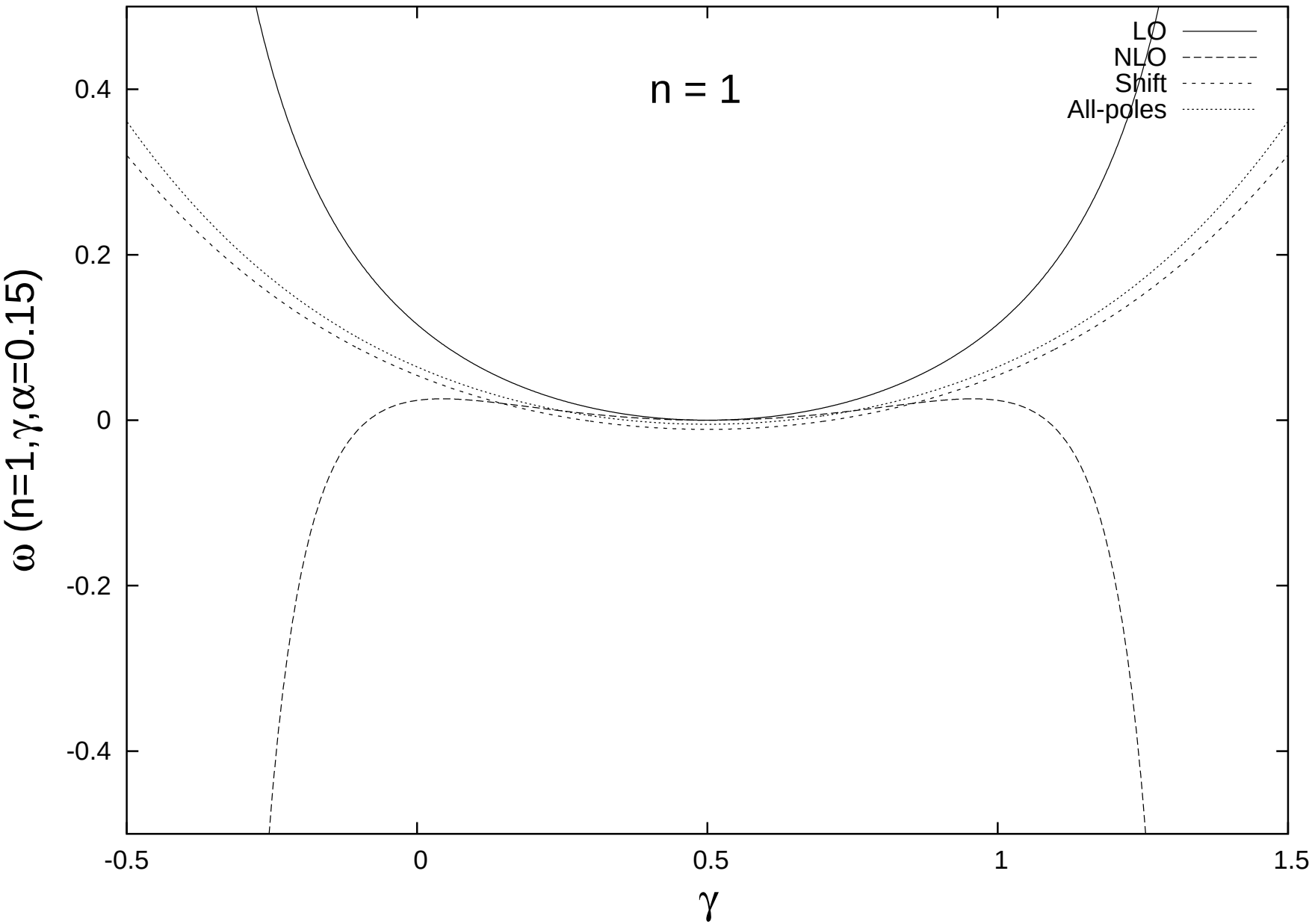
n = 1
LO
NLO
Shift
All-poles
0.4
0.2
0
-0.2
-0.4
-0.5
0
0.5
1
1.5
γ
ω (n=1,γ,α=0.15)

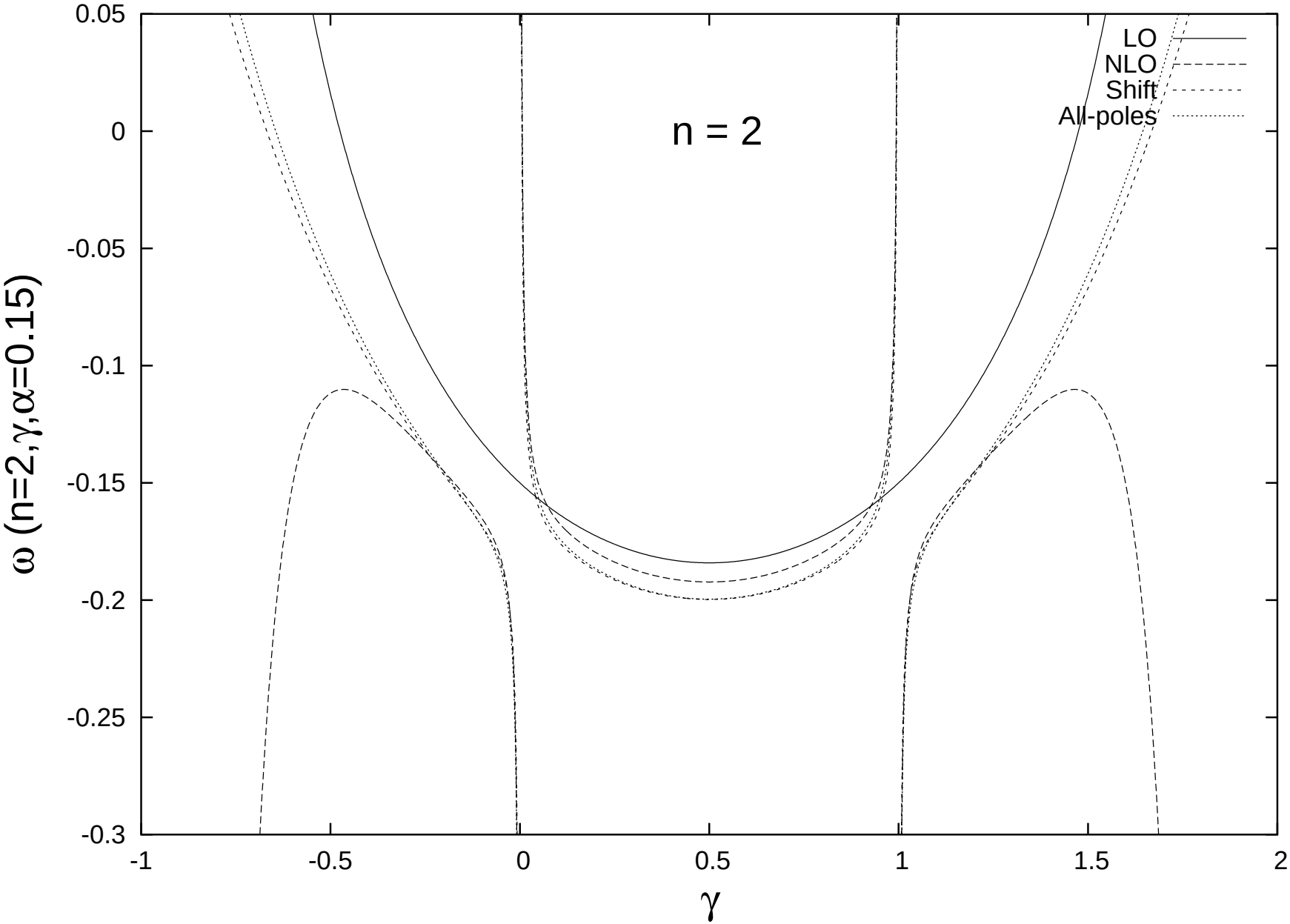
n = 2
LO
NLO
Shift
All-poles
ω (n=2,γ,α=0.15)
γ
0.05
0
-0.05
-0.1
-0.15
-0.2
-0.25
-0.3
-1
-0.5
0
0.5
1
1.5
2

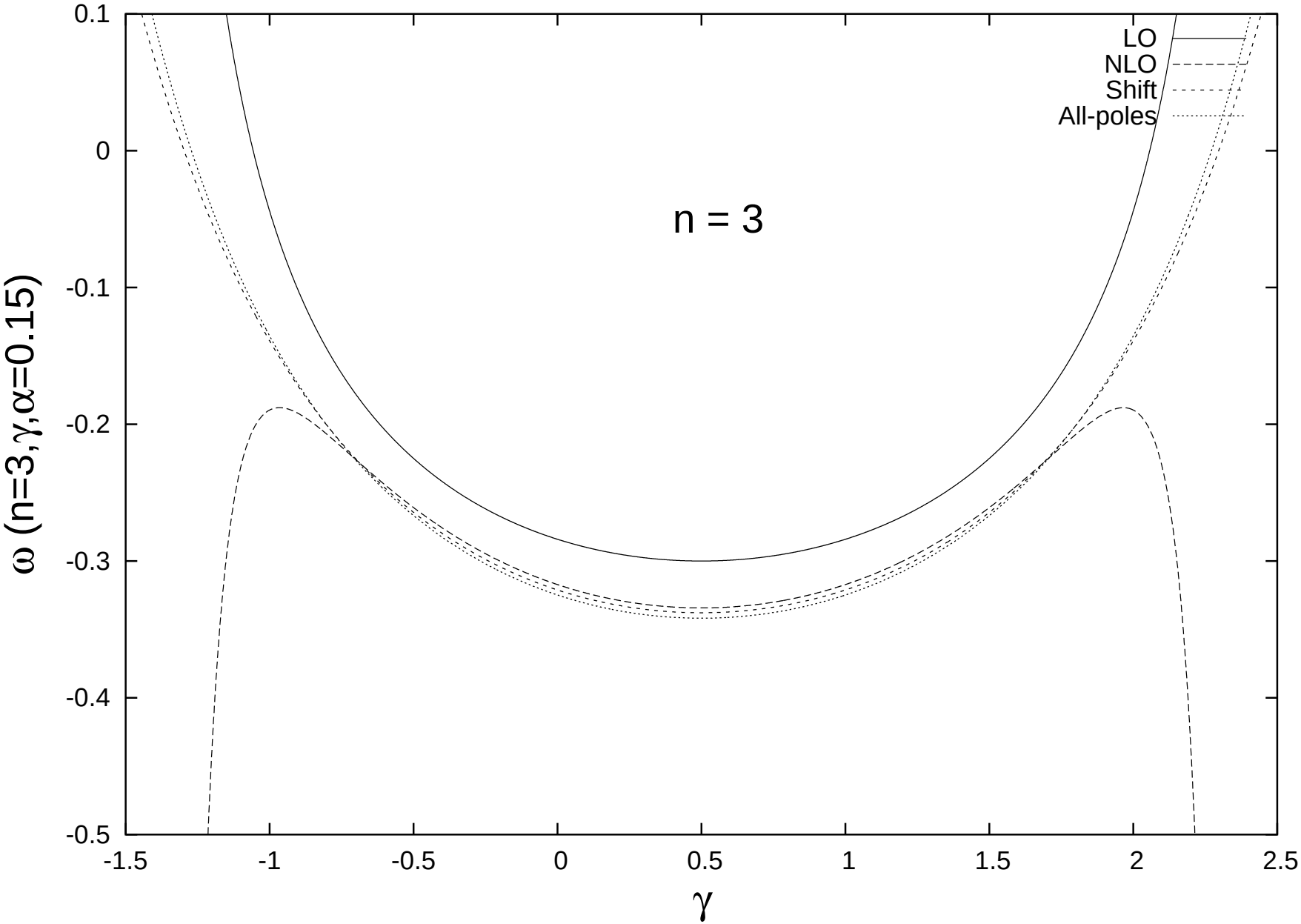
LO
NLO
Shift
All-poles
n = 3
ω (n=3,γ,α=0.15)
γ
0.1
0
-0.1
-0.2
-0.3
-0.4
-0.5
-1.5
-1
-0.5
0
0.5
1
1.5
2
2.5

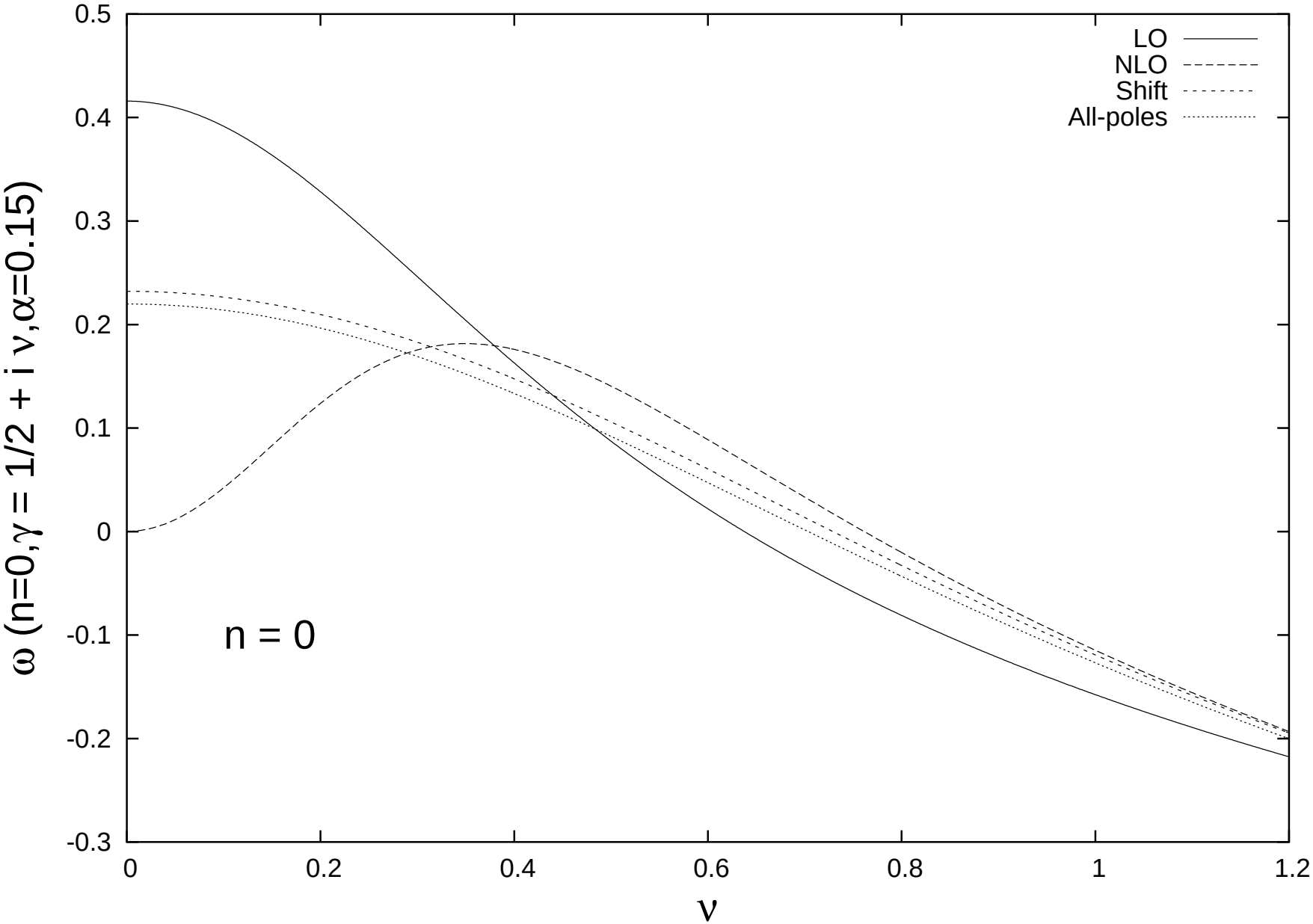
LO
NLO
Shift
All-poles
n = 0
ω (n=0,γ = 1/2 + i ν,α=0.15)
ν
0.5
0.4
0.3
0.2
0.1
0
-0.1
-0.2
-0.3
0
0.2
0.4
0.6
0.8
1
1.2

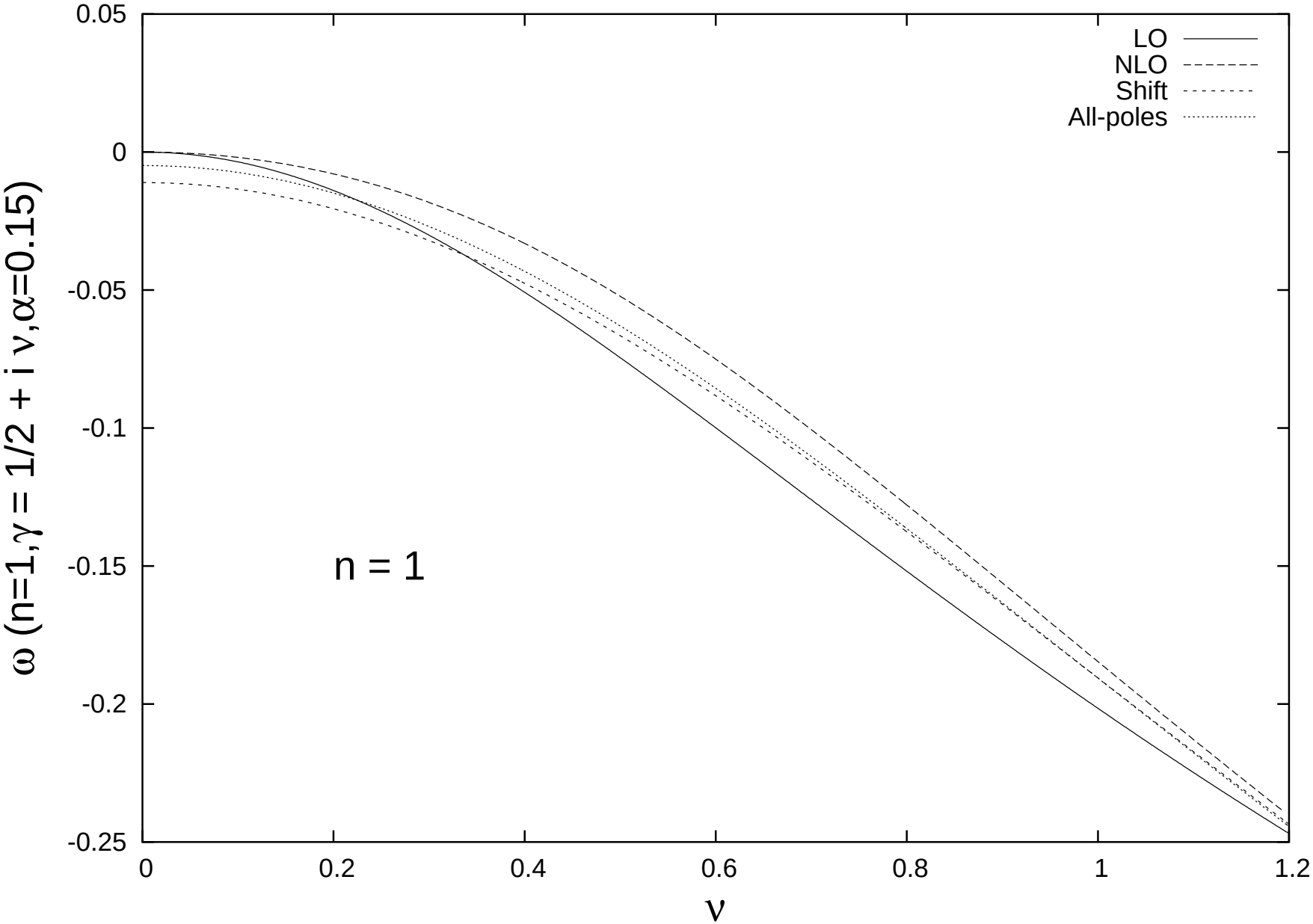
LO
NLO
Shift
All-poles
n = 1
ω (n=1,γ = 1/2 + i ν,α=0.15)
ν
0.05
0
-0.05
-0.1
-0.15
-0.2
-0.25
0
0.2
0.4
0.6
0.8
1
1.2

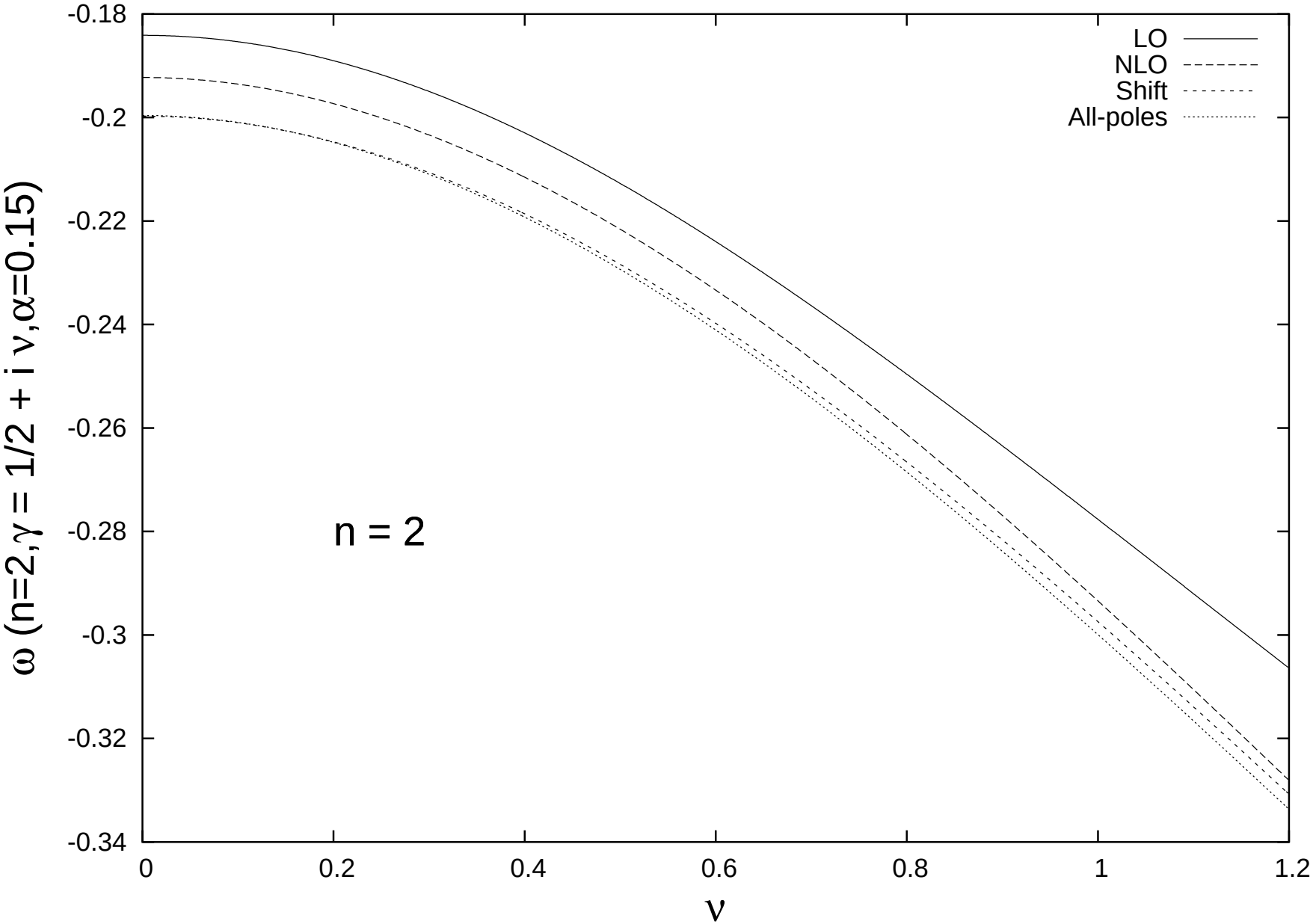
LO
NLO
Shift
All-poles
n = 2
ω (n=2,γ = 1/2 + i ν,α=0.15)
ν
-0.18
-0.2
-0.22
-0.24
-0.26
-0.28
-0.3
-0.32
-0.34
0
0.2
0.4
0.6
0.8
1
1.2

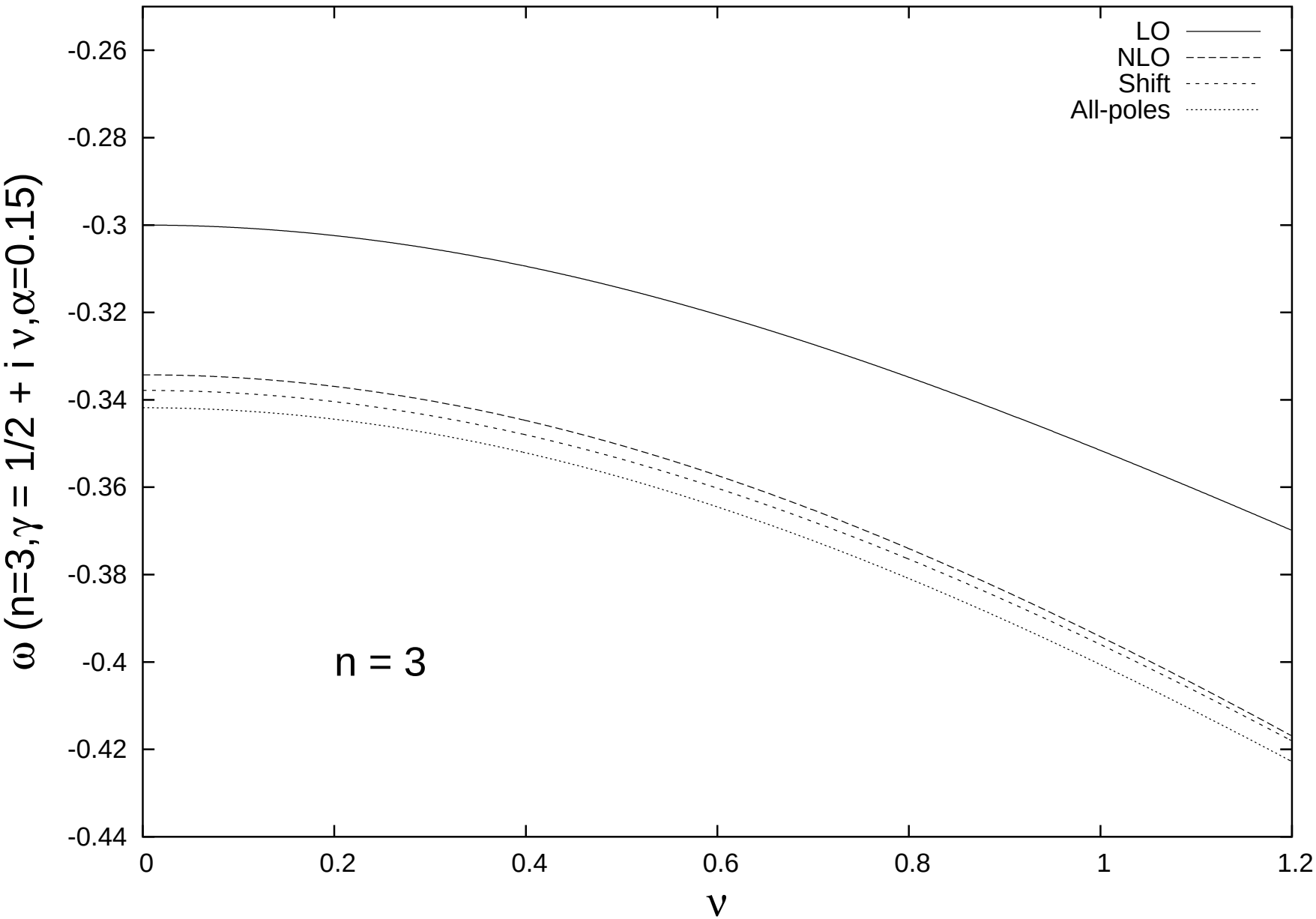
LO
NLO
Shift
All-poles
n = 3
ω (n=3,γ = 1/2 + i ν,α=0.15)
ν
-0.26
-0.28
-0.3
-0.32
-0.34
-0.36
-0.38
-0.4
-0.42
-0.44
0
0.2
0.4
0.6
0.8
1
1.2

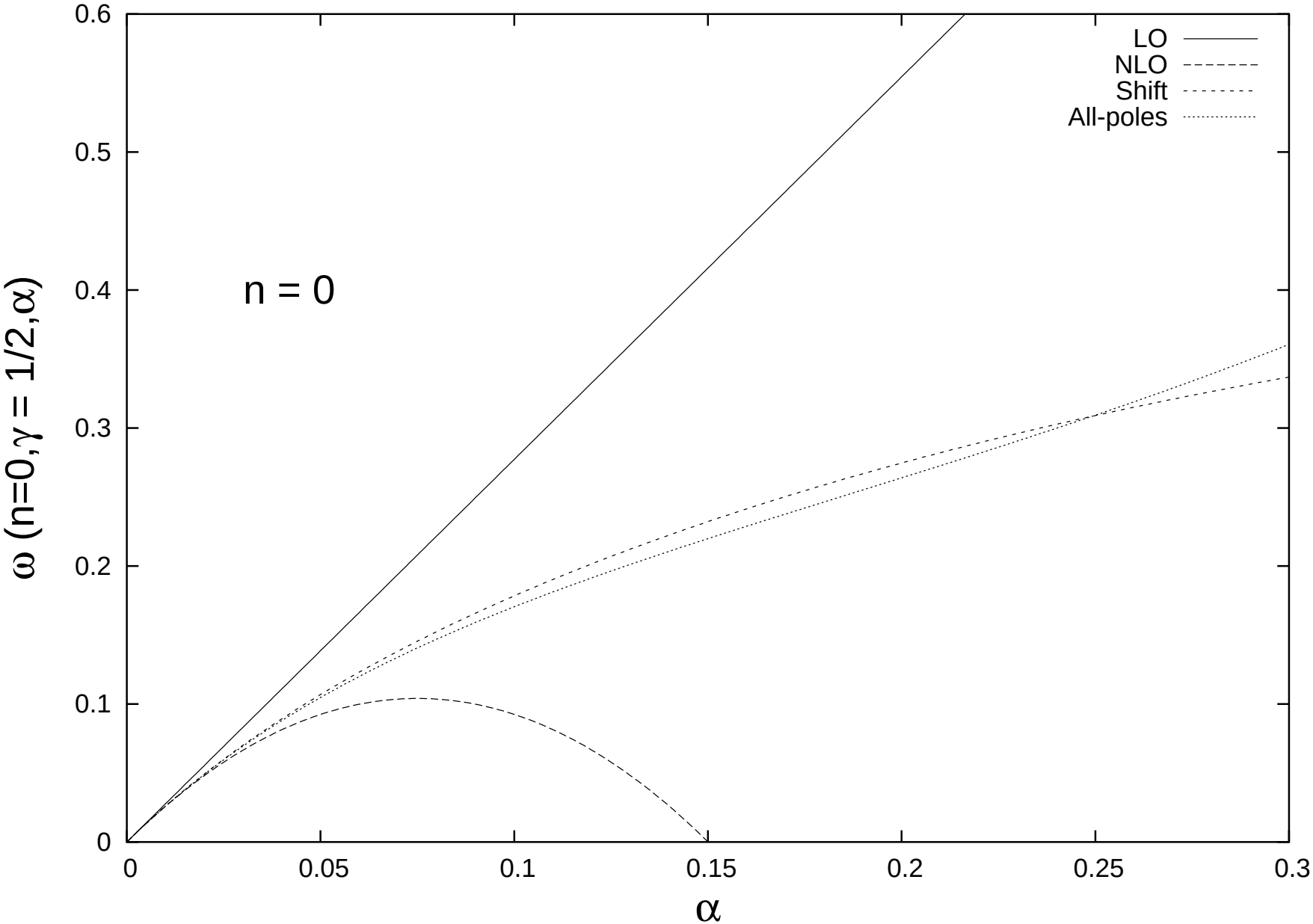
LO
NLO
Shift
All-poles
n = 0
ω (n=0,γ = 1/2,α)
α
0
0.1
0.2
0.3
0.4
0.5
0.6
0
0.05
0.1
0.15
0.2
0.25
0.3

Mueller and Navelet proposed this process as ideal to apply the BFKL formalism and predicted a power–like rise for the cross section. However, to realize this growth as a manifestation of multi–Regge kinematics is very difficult since it is drastically damped by the behavior of the parton distribution functions for $x \to 1$.

The DØ collaboration analyzed data taken at the Tevatron $p\bar{p}$–collider from two periods of measurement at different energies $\sqrt{s} = 630$ and 1800 GeV. From these they extracted an intercept of $1.65 \pm .07$. This rise is even faster than that predicted in the LO BFKL calculation which for the kinematics relevant in the DØ experiment yields an approximated value of 1.45.

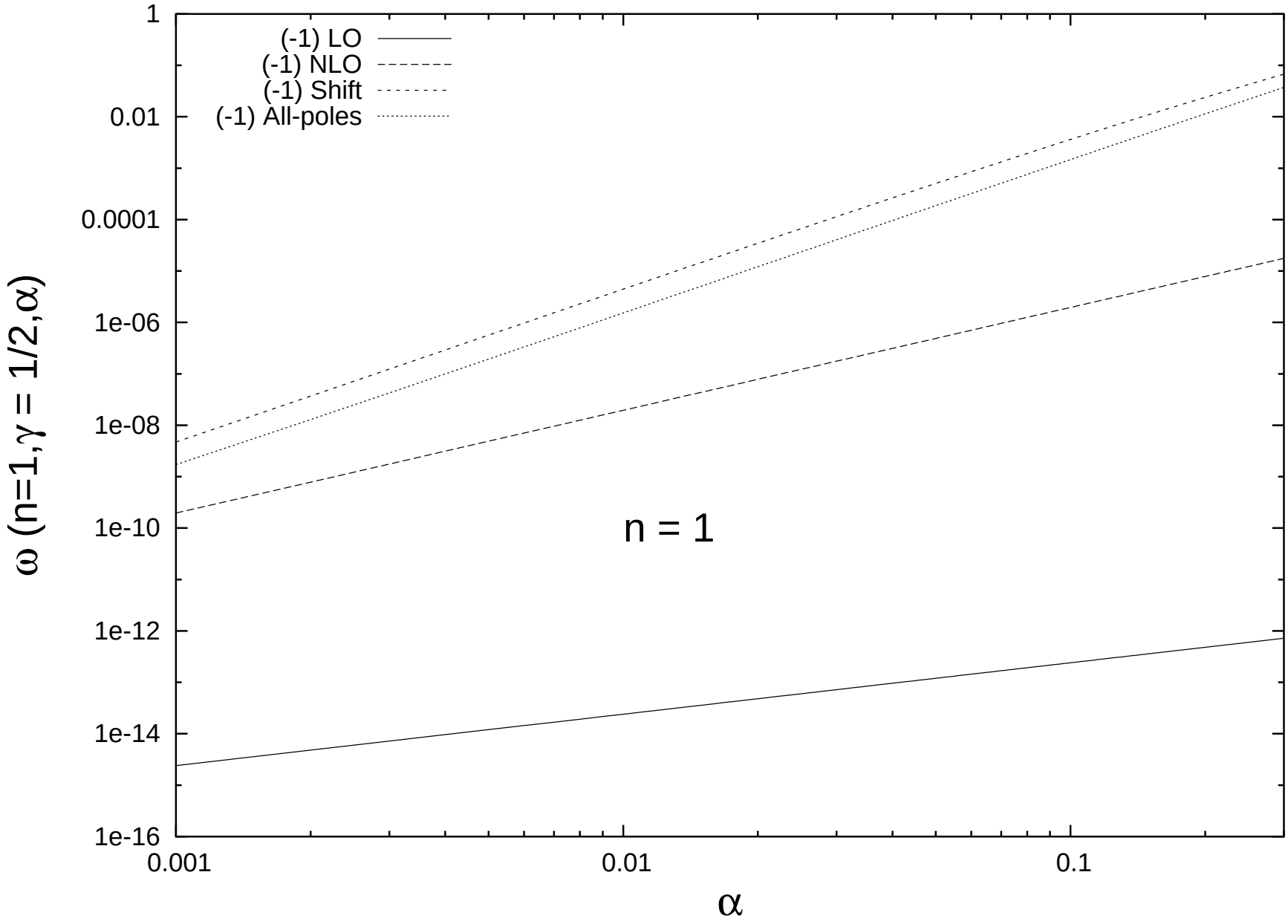
(-1) LO
(-1) NLO
(-1) Shift
(-1) All-poles
n = 1
ω (n=1,γ = 1/2,α)
α
1
0.01
0.0001
1e-06
1e-08
1e-10
1e-12
1e-14
1e-16
0.001
0.01
0.1

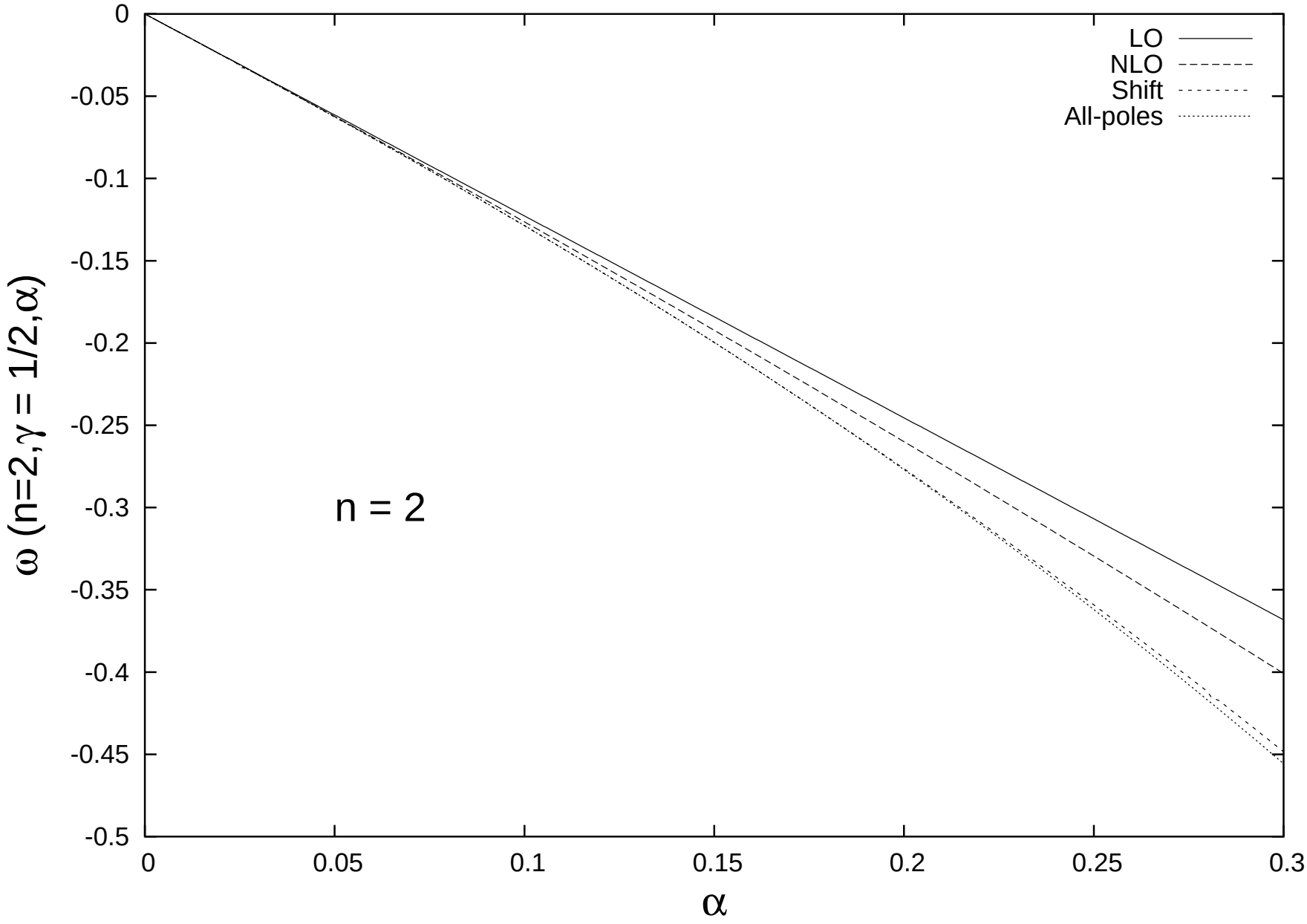
LO
NLO
Shift
All-poles
n = 2
ω (n=2,γ = 1/2,α)
α
0
-0.05
-0.1
-0.15
-0.2
-0.25
-0.3
-0.35
-0.4
-0.45
-0.5
0
0.05
0.1
0.15
0.2
0.25
0.3

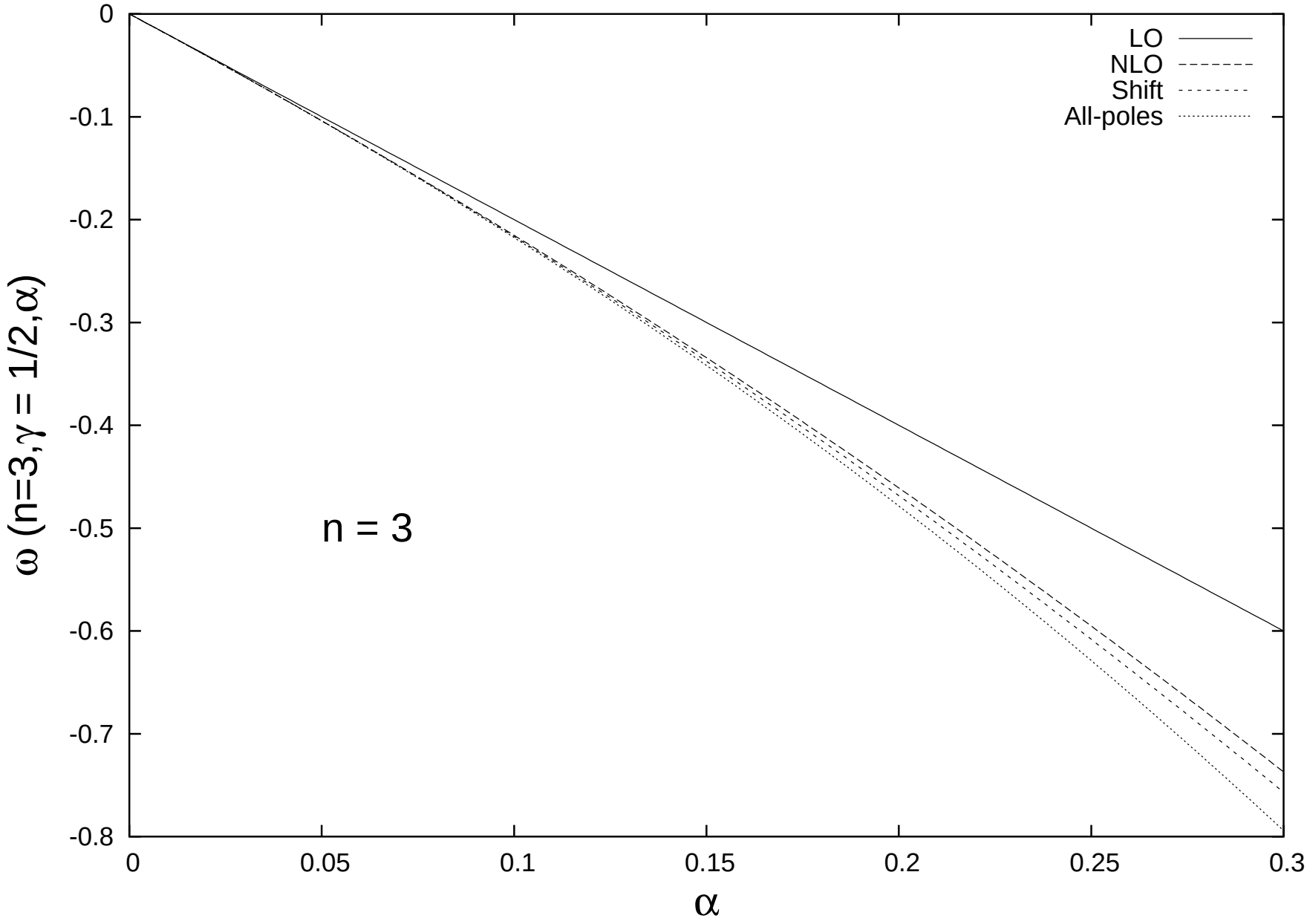
LO
NLO
Shift
All-poles
n = 3
ω (n=3,γ = 1/2,α)
α
0
-0.1
-0.2
-0.3
-0.4
-0.5
-0.6
-0.7
-0.8
0
0.05
0.1
0.15
0.2
0.25
0.3

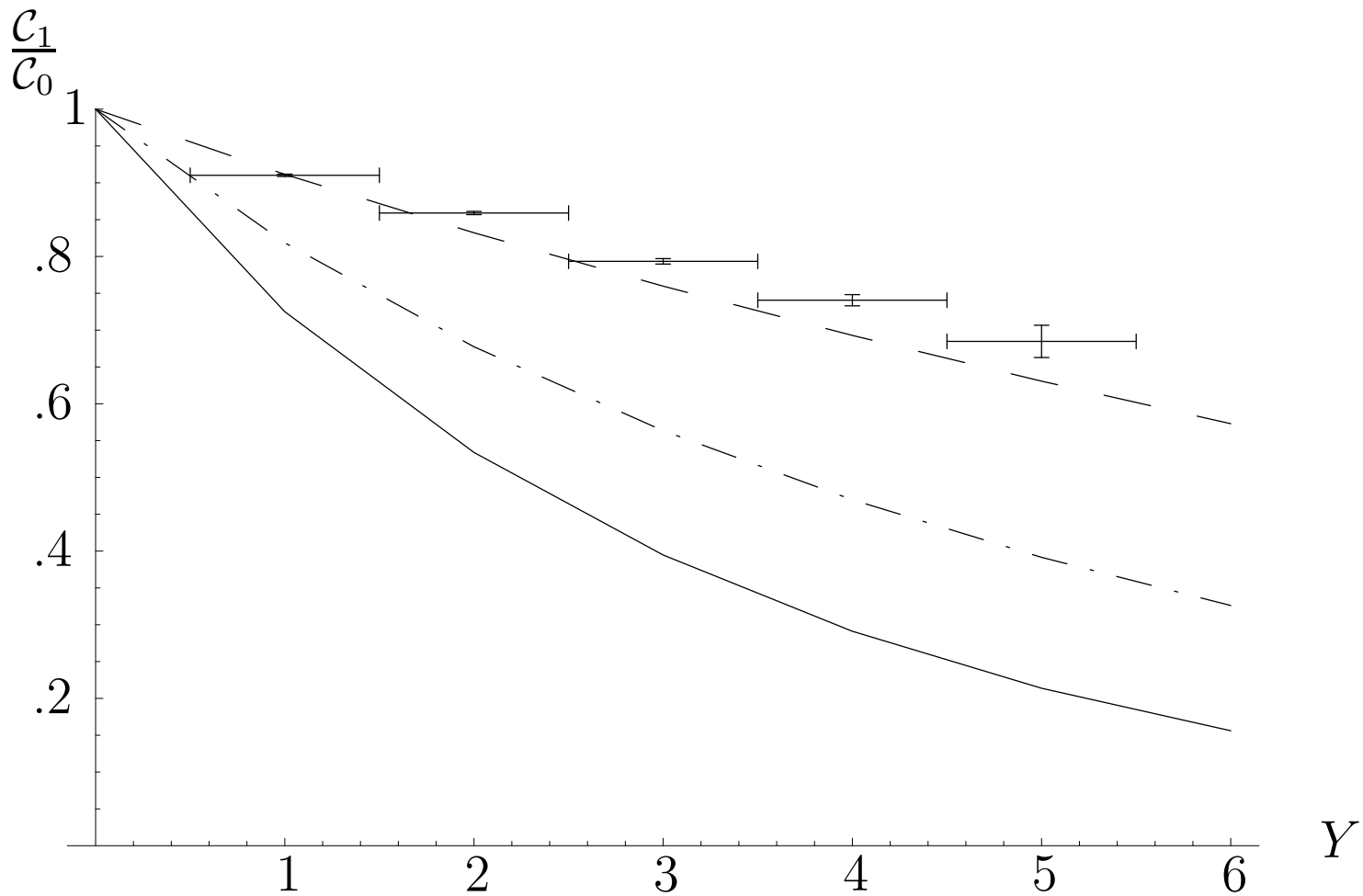

Figure 2: $\langle \cos\phi \rangle = \mathcal{C}_1/\mathcal{C}_0$ at a $p\bar{p}$ collider with $\sqrt{s} = 1.8$ TeV for BFKL at LO (solid), NLO (dashed), and collinear resummation (dash–dotted).

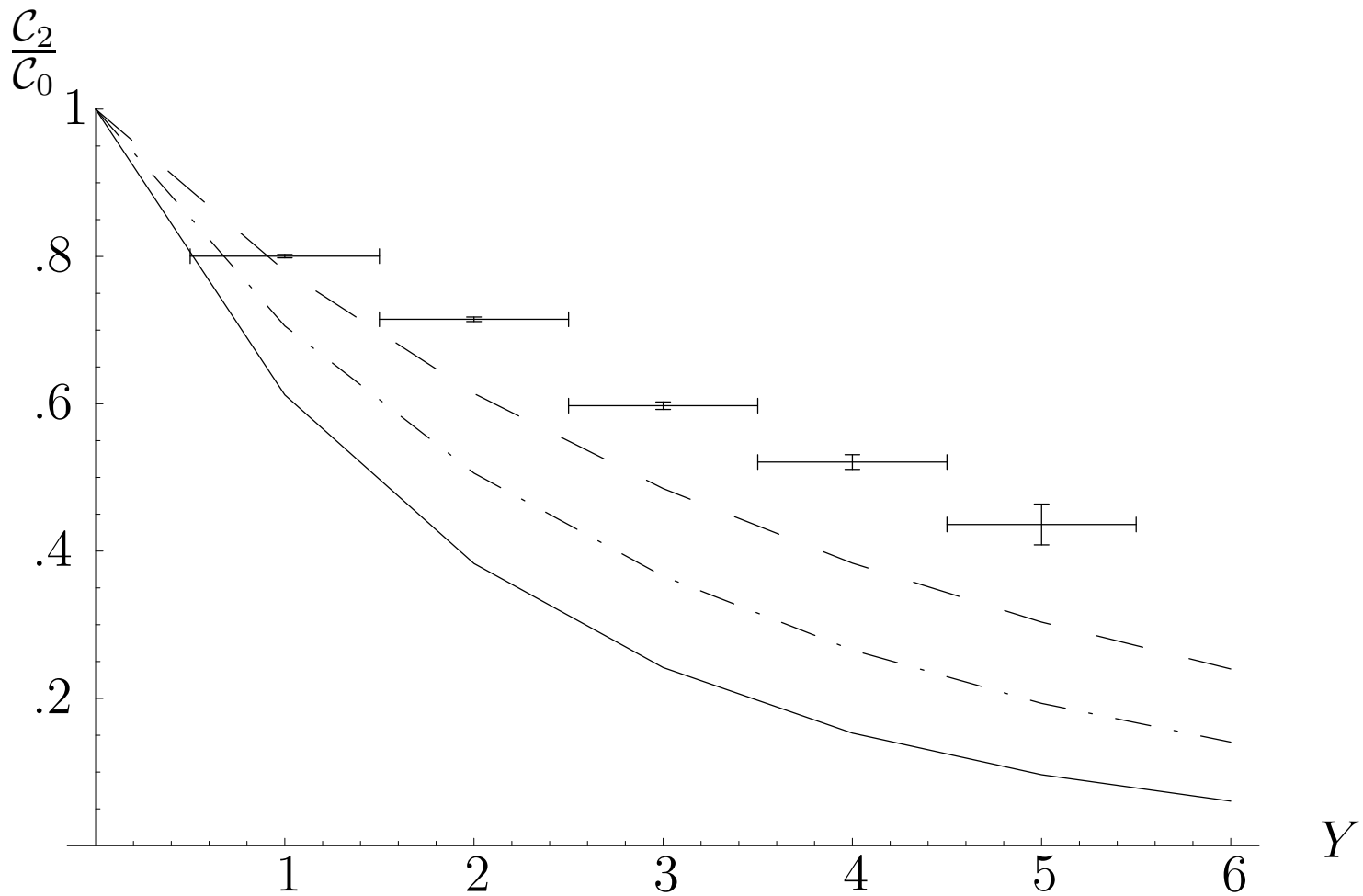

Figure 3: $\langle \cos 2\phi \rangle = \mathcal{C}_2/\mathcal{C}_0$ at a $p\bar{p}$ collider with $\sqrt{s} = 1.8$ TeV for BFKL at LO (solid), NLO (dashed), and collinear resummation (dash–dotted).

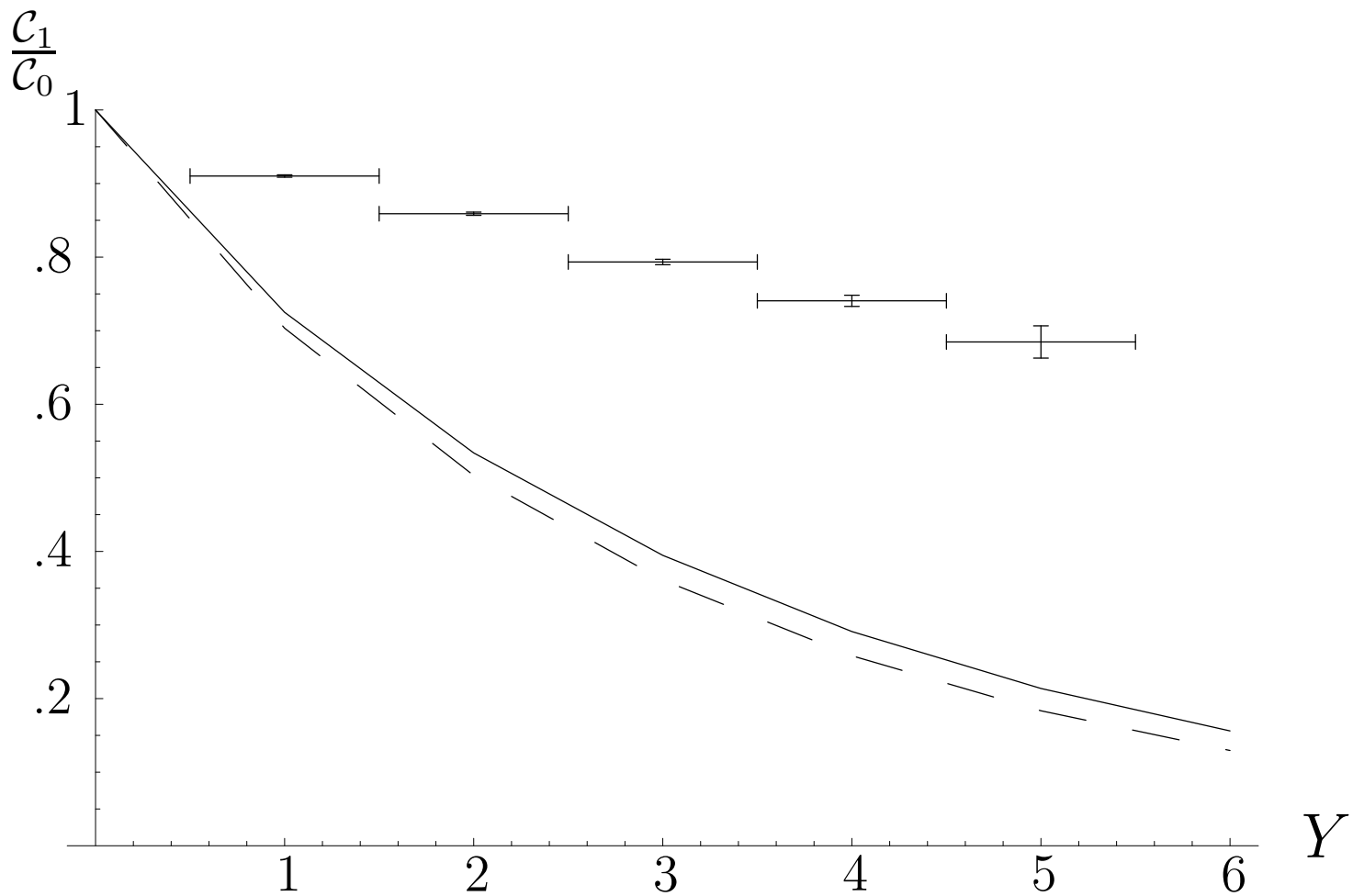

Figure 4: $\langle \cos\phi \rangle$ at LO comparing the $\overline{\mathrm{MS}}$ renormalization scheme (solid) with the GB scheme (dashed).

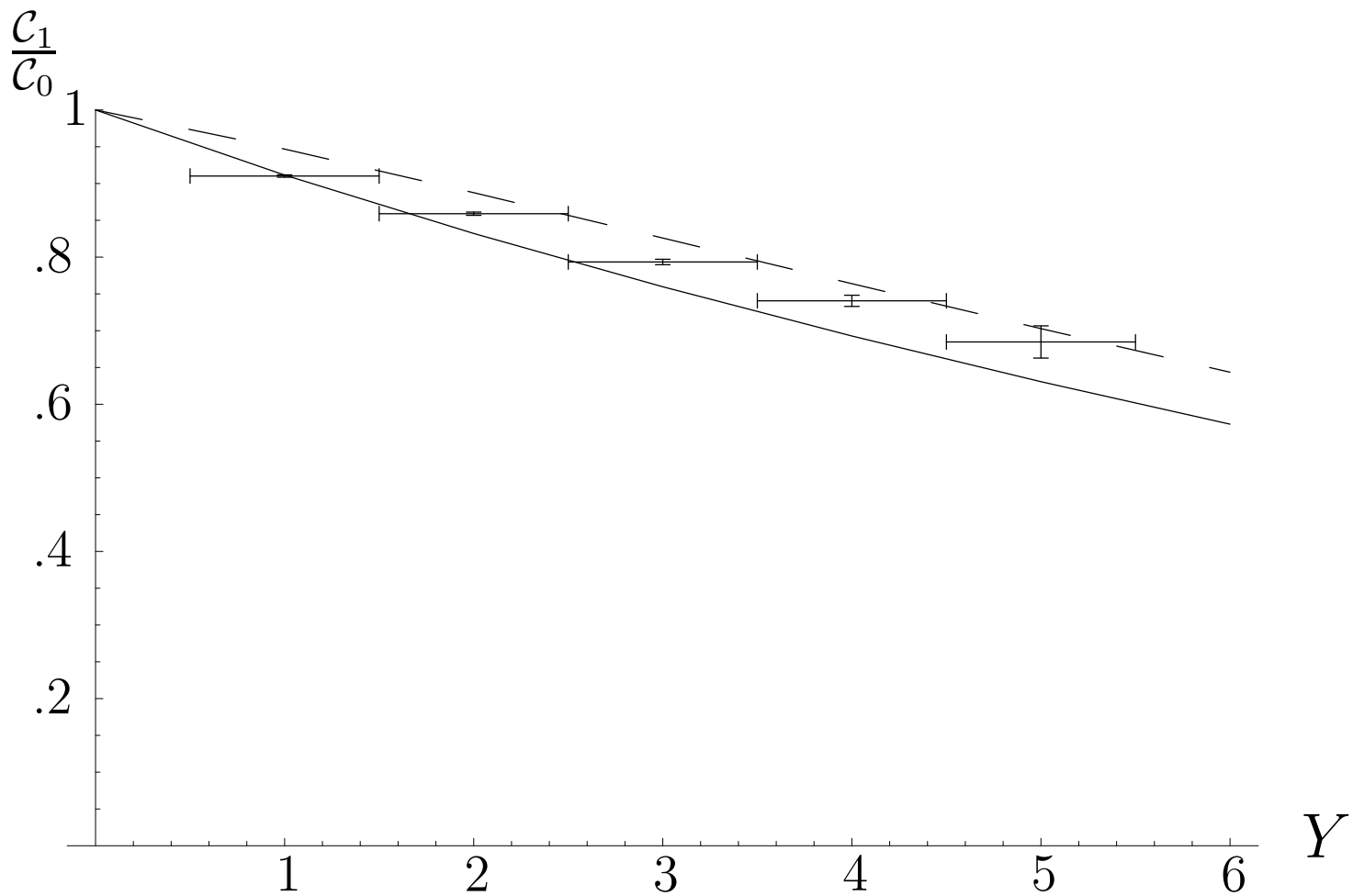

Figure 5: $\langle \cos\phi \rangle$ at NLO comparing the $\overline{\mathrm{MS}}$ renormalization scheme (solid) with the GB scheme (dashed).

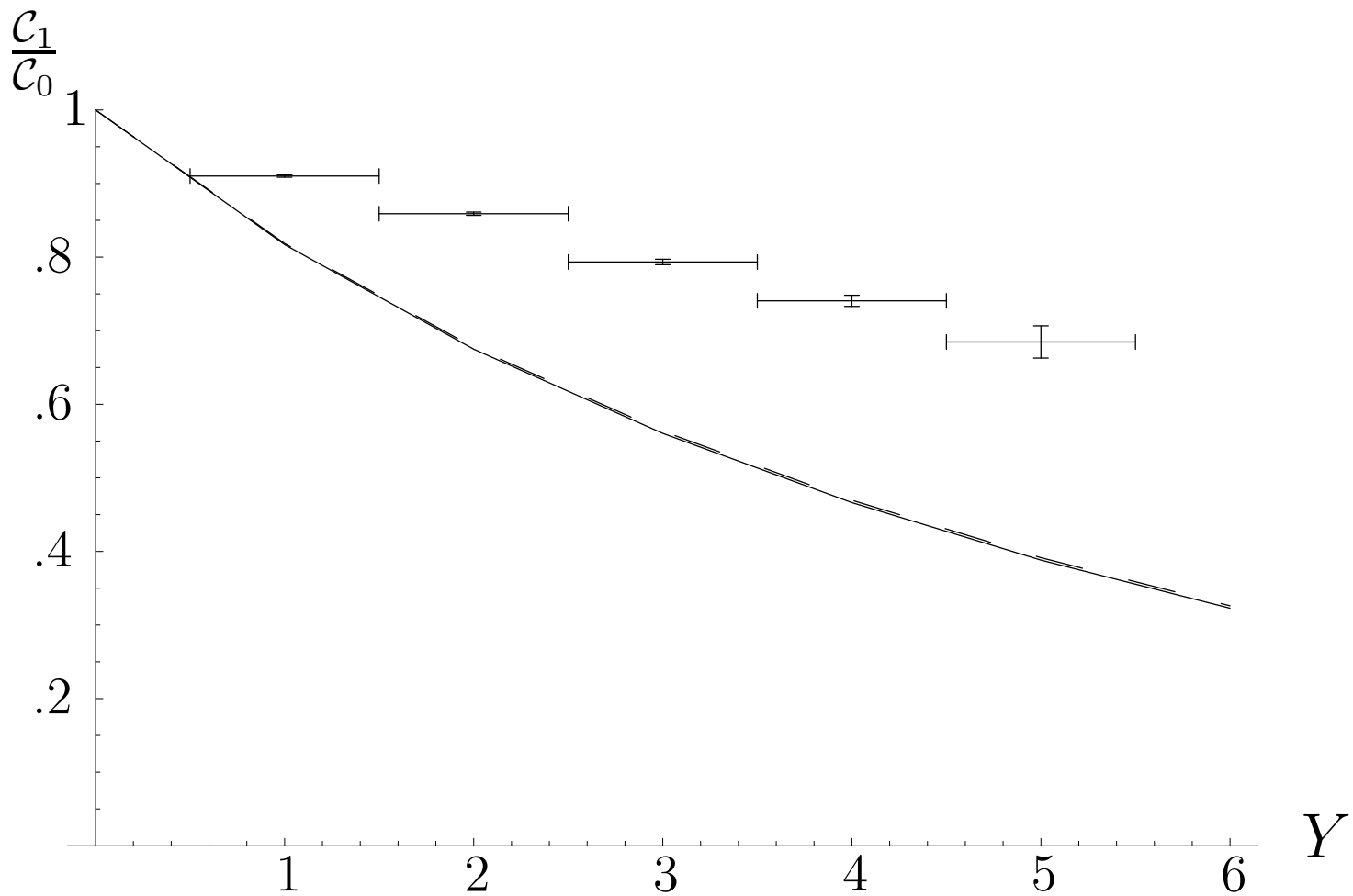

Figure 6: $\langle \cos\phi \rangle$ with a resummed kernel comparing the $\overline{\mathrm{MS}}$ renormalization scheme (solid) with the GB scheme (dashed).

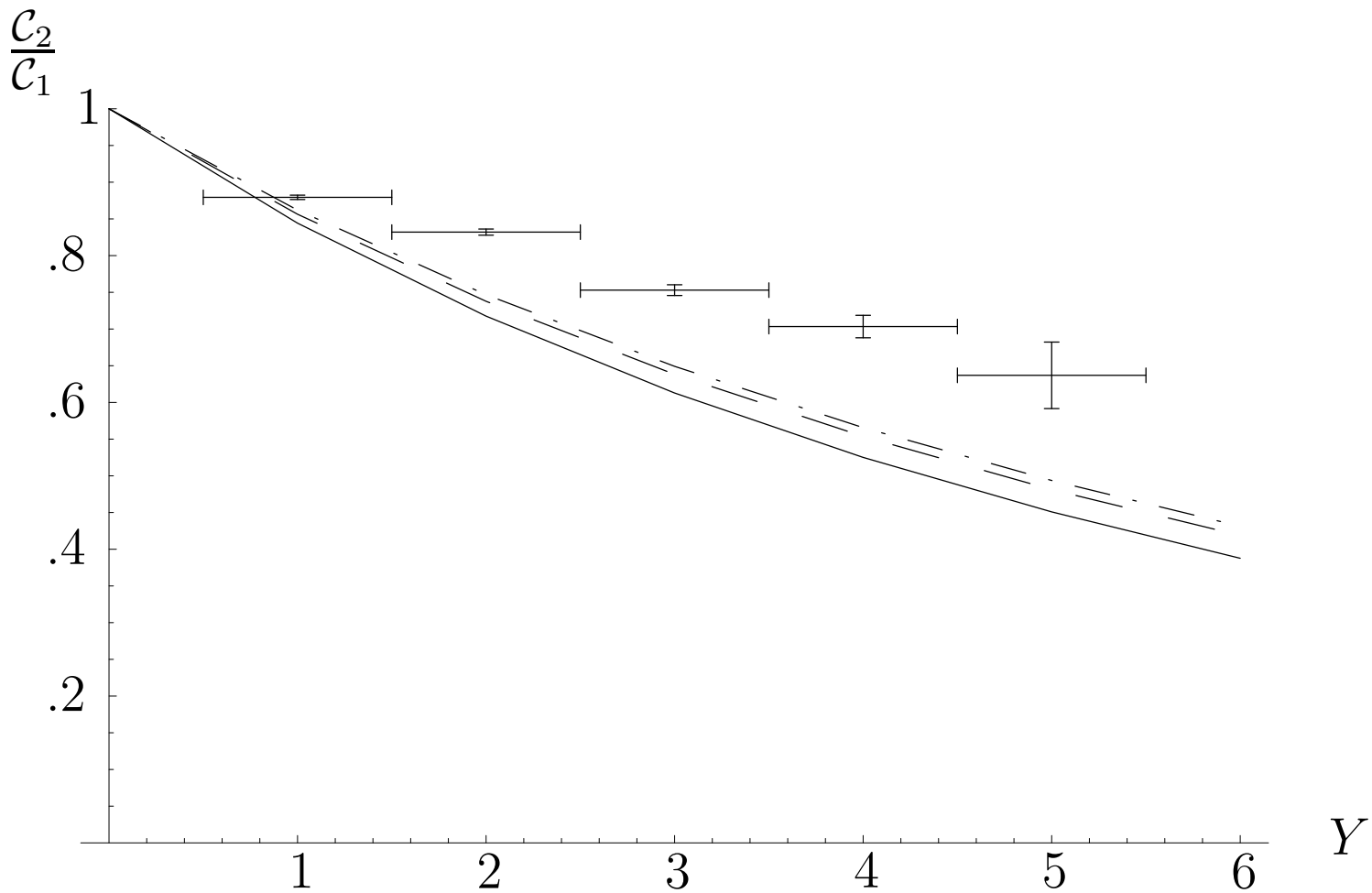

Figure 7: $\frac{<\cos 2\phi>}{<\cos\phi>} = \frac{\mathcal{C}_2}{\mathcal{C}_1}$ with LO (solid), NLO (dashed) and collinearly resummed (dash-dotted) BFKL kernels.

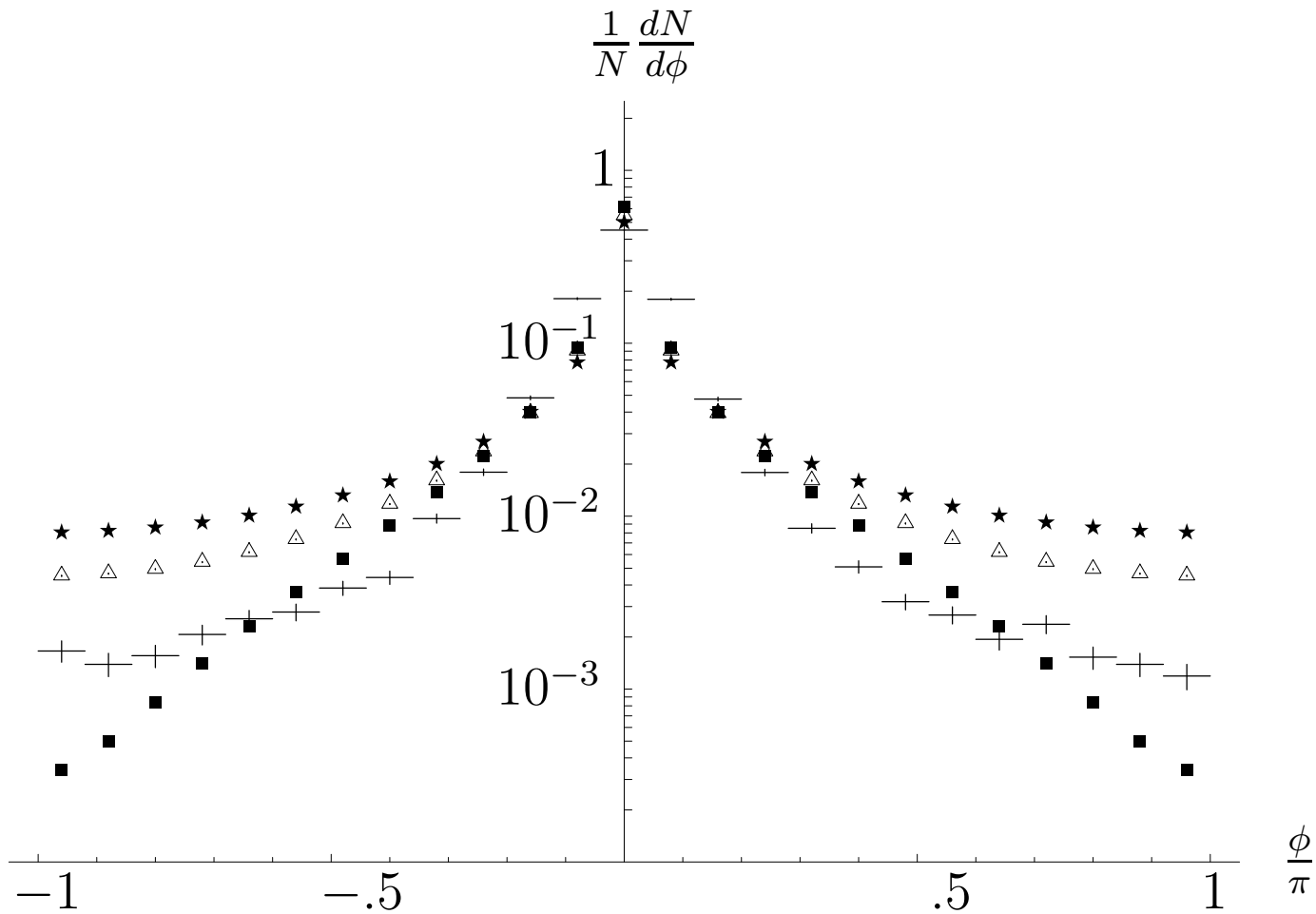

Figure 8: $\frac{1}{N}\frac{dN}{d\phi}$ in a $p\bar{p}$ collider at $\sqrt{s}$=1.8 TeV using a LO (stars), NLO (squares) and resummed (triangles) BFKL kernel, for Y = 1.

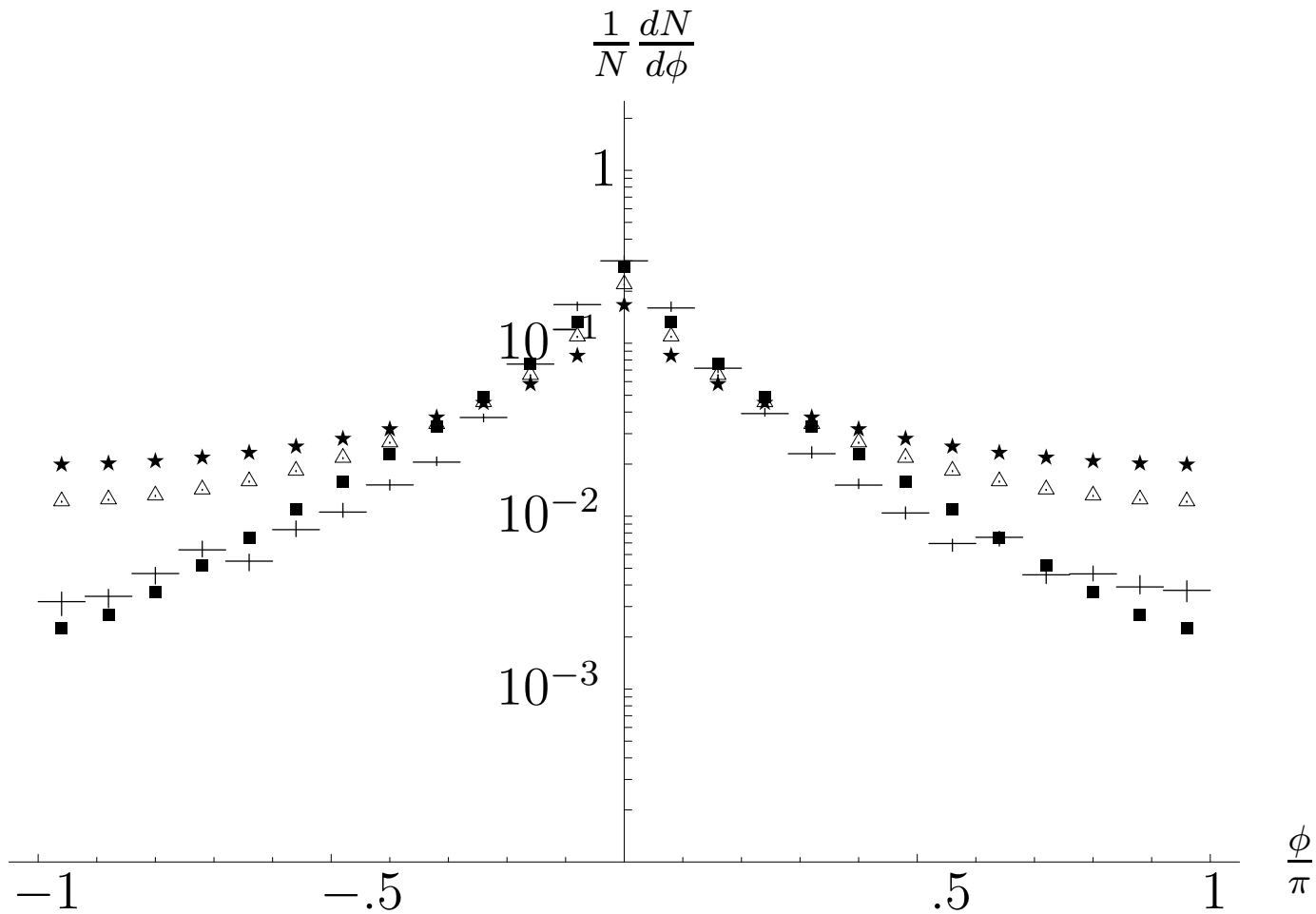

Figure 9: $\frac{1}{N}\frac{dN}{d\phi}$ in a $p\bar{p}$ collider at $\sqrt{s}$=1.8 TeV using a LO (stars), NLO (squares) and resummed (triangles) BFKL kernel, for Y = 3.

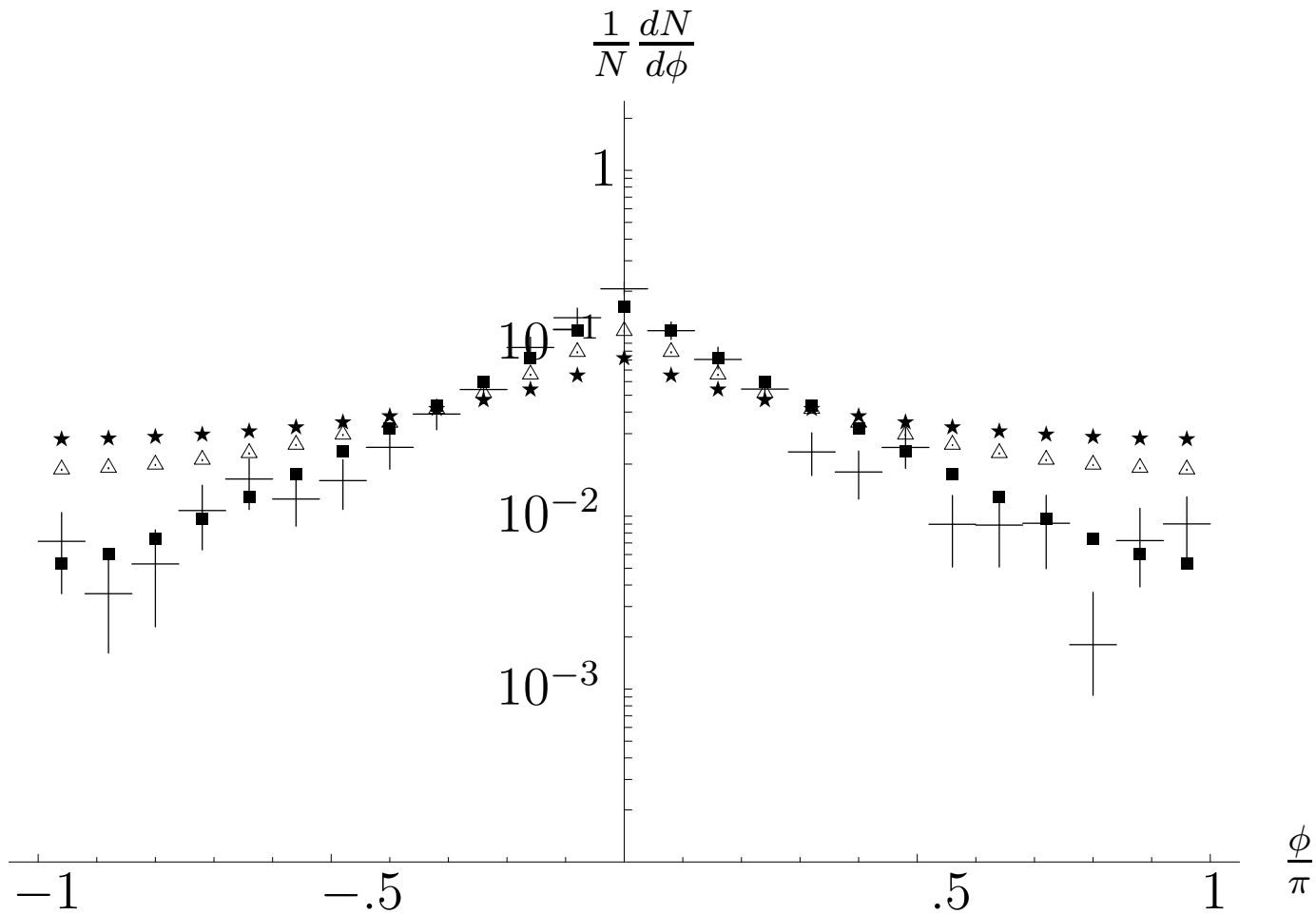

Figure 10: $\frac{1}{N}\frac{dN}{d\phi}$ in a $p\bar{p}$ collider at $\sqrt{s}$=1.8 TeV using a LO (stars), NLO (squares) and resummed (triangles) BFKL kernel, for Y = 5.

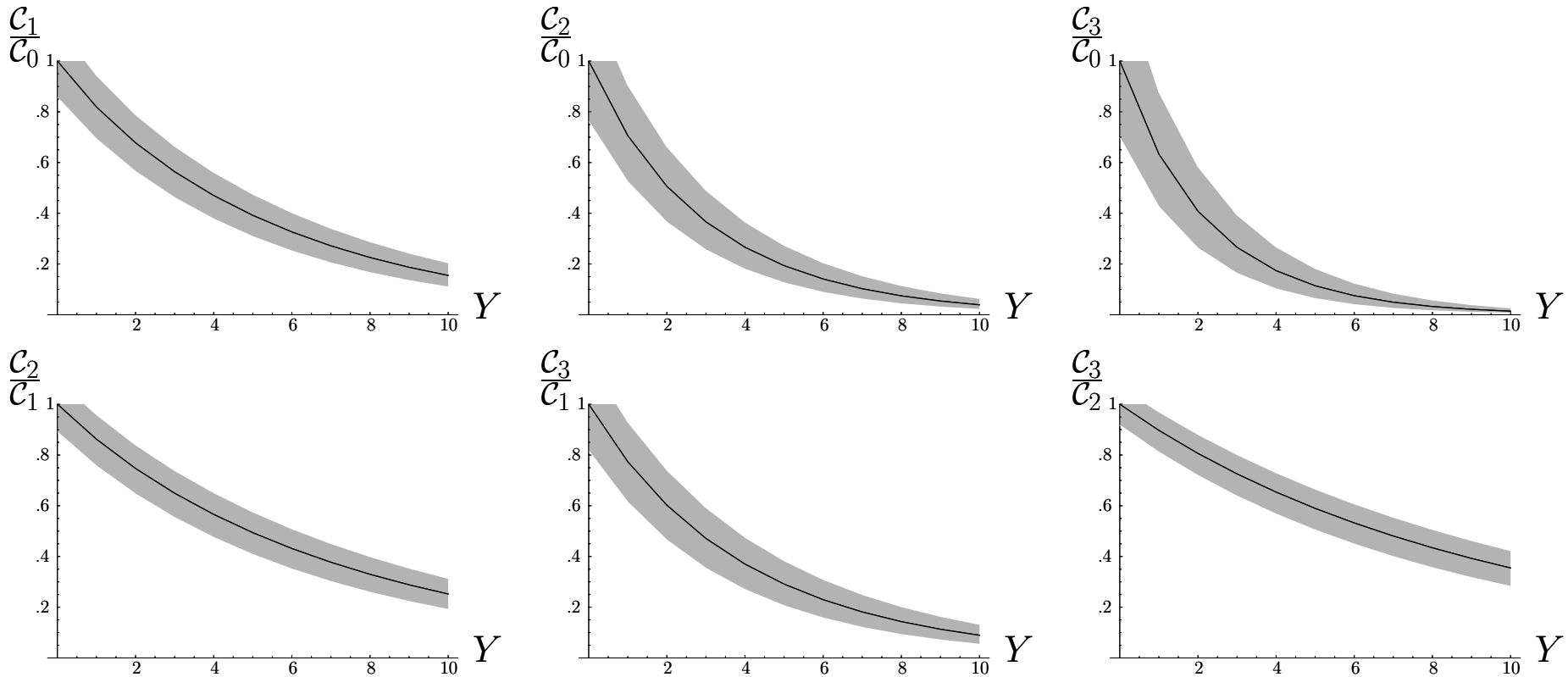

Figure 11: Different ratios of the coefficients $\mathcal{C}_n$ obtained using a collinearly resummed BFKL kernel. The gray band reflects the uncertainty in s_0 and in the renormalization scale μ.

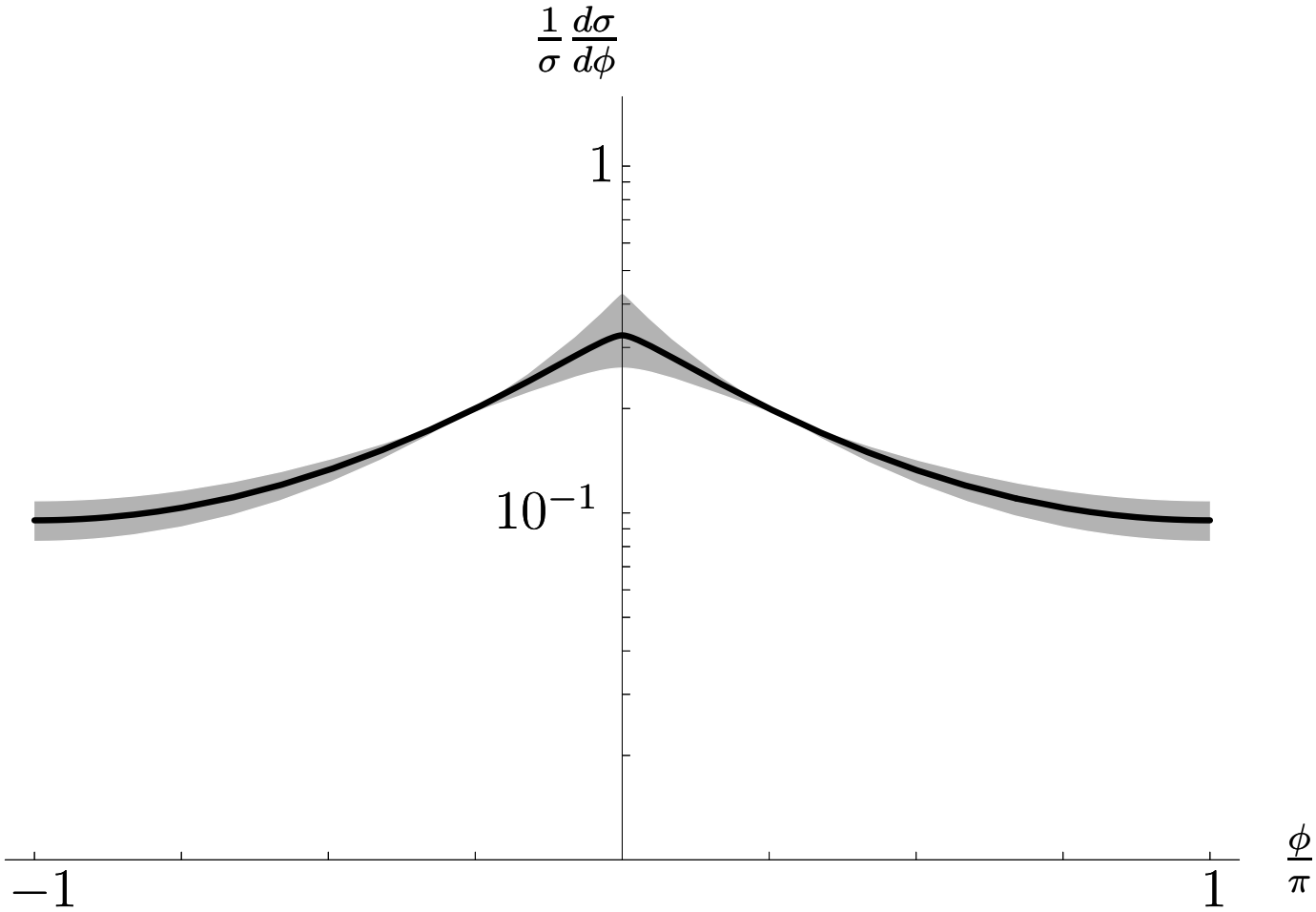

Figure 12: $\frac{1}{\sigma}\frac{d\sigma}{d\phi}$ in our resummation scheme for rapidities Y = 7. The gray band reflects the uncertainty in s_0 and in the renormalization scale μ.

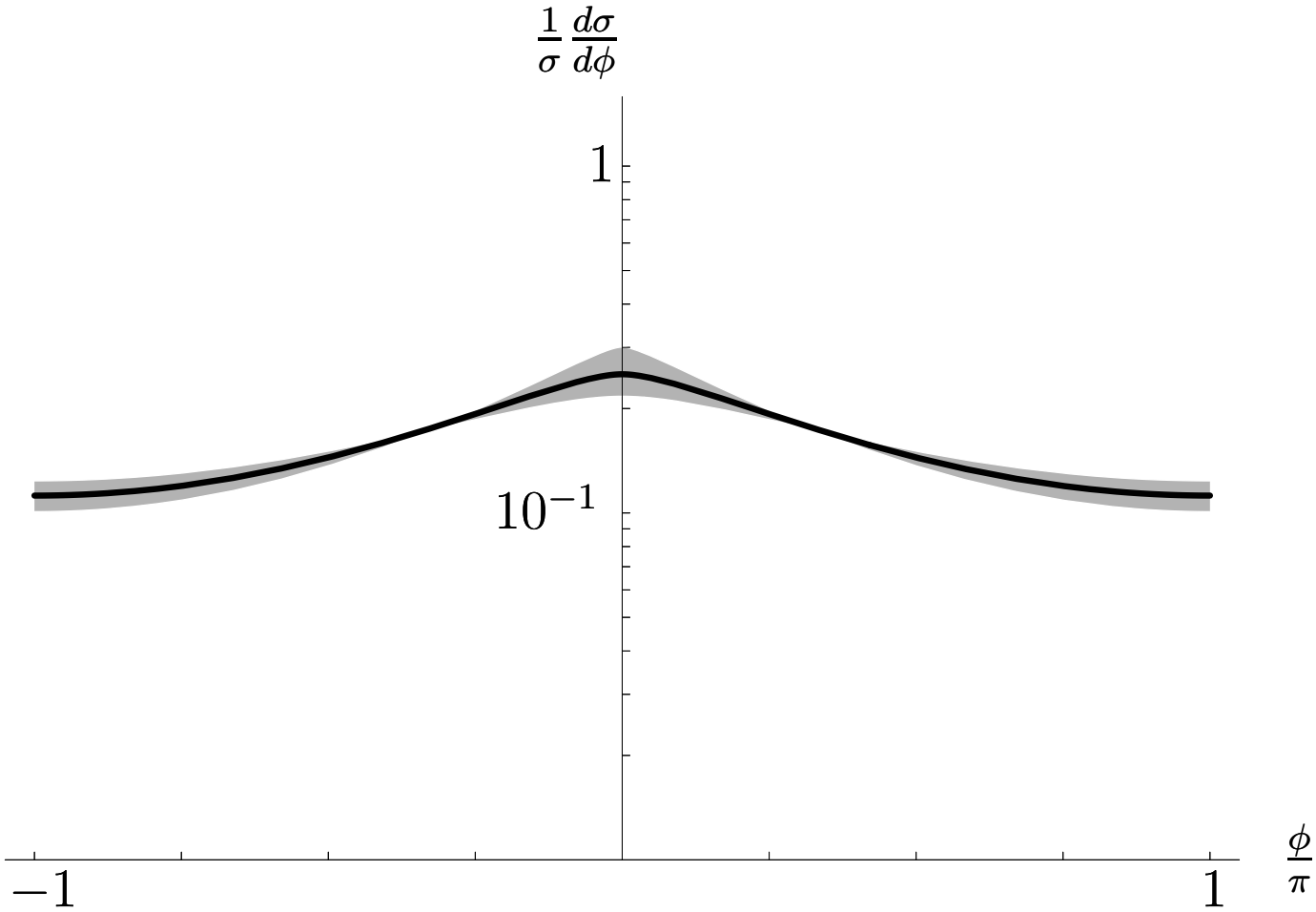

Figure 13: $\frac{1}{\sigma}\frac{d\sigma}{d\phi}$ in our resummation scheme for rapidities Y = 9. The gray band reflects the uncertainty in s_0 and in the renormalization scale μ.

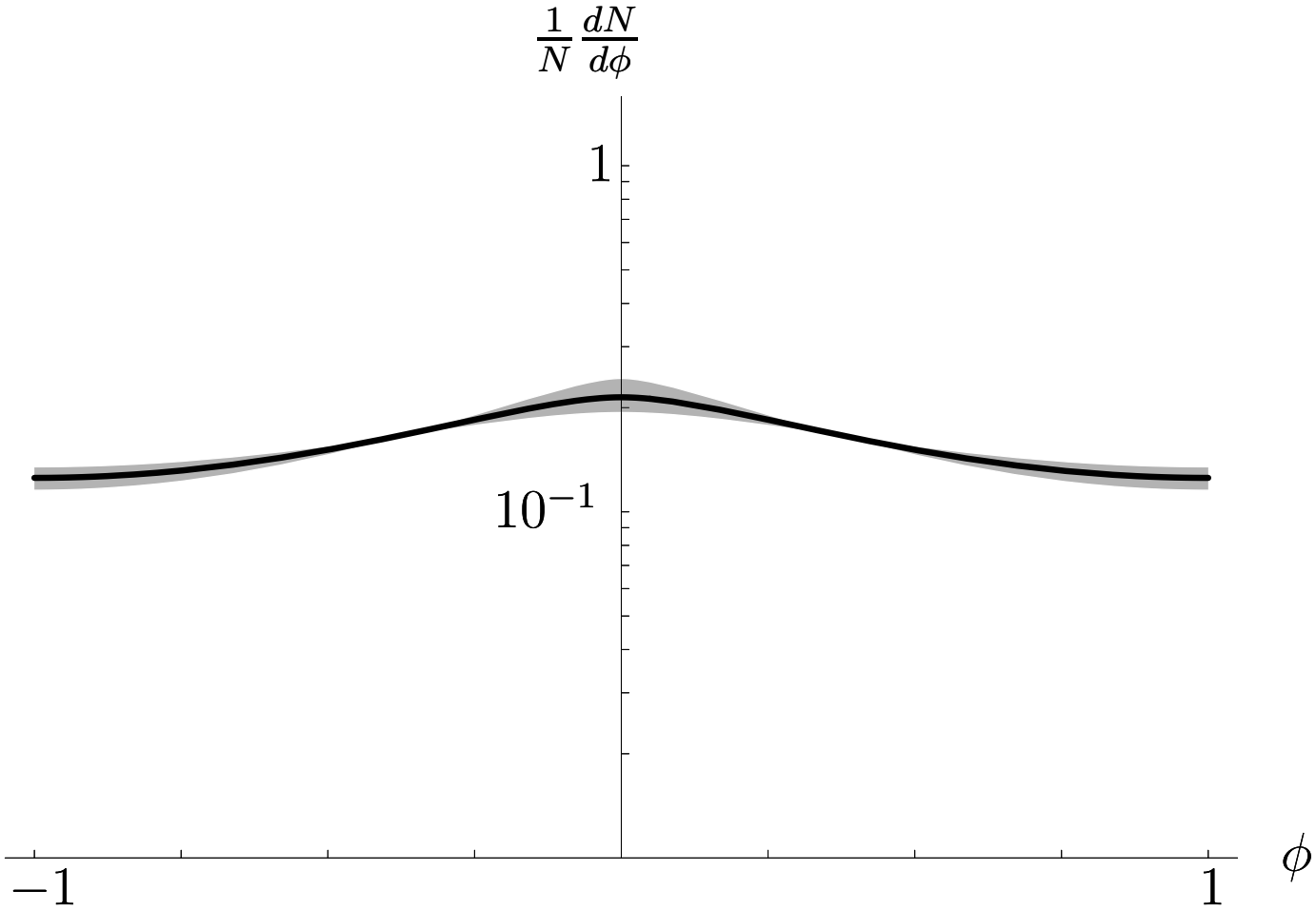

Figure 14: $\frac{1}{\sigma}\frac{d\sigma}{d\phi}$ in our resummation scheme for rapidities Y = 11. The gray band reflects the uncertainty in s_0 and in the renormalization scale μ.

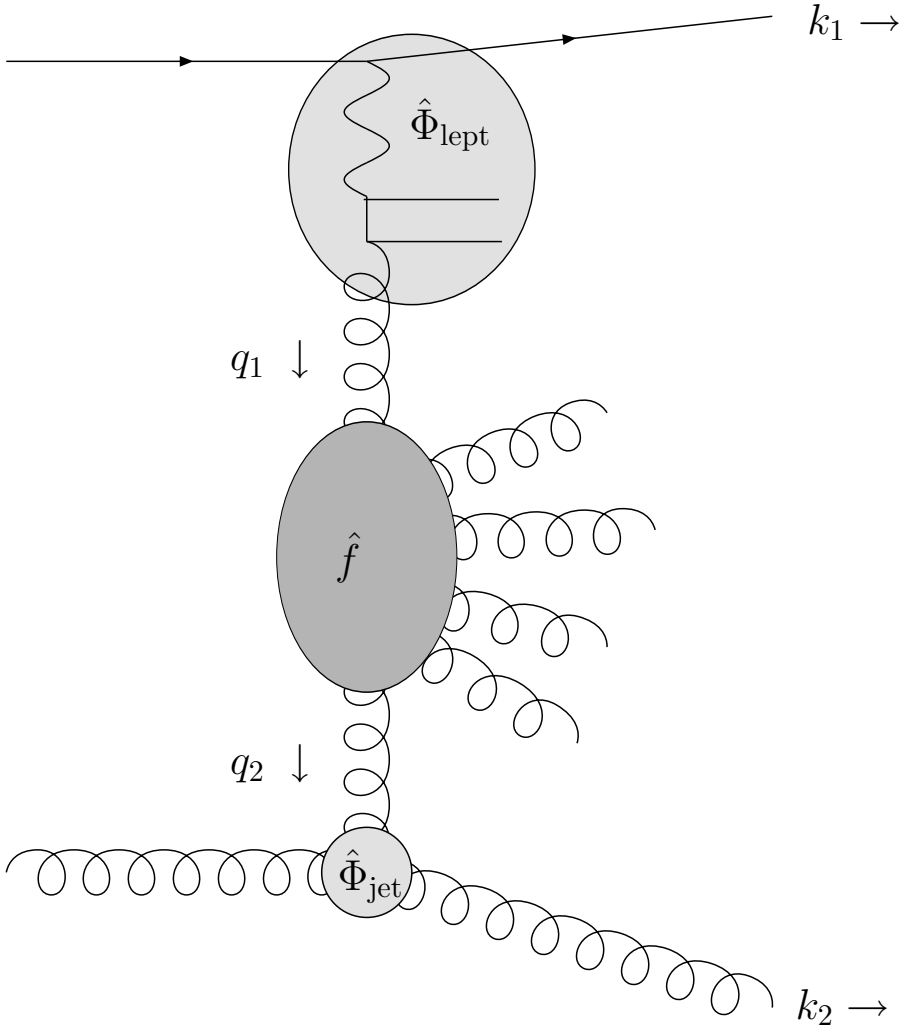

Figure 15: Forward jet production in DIS

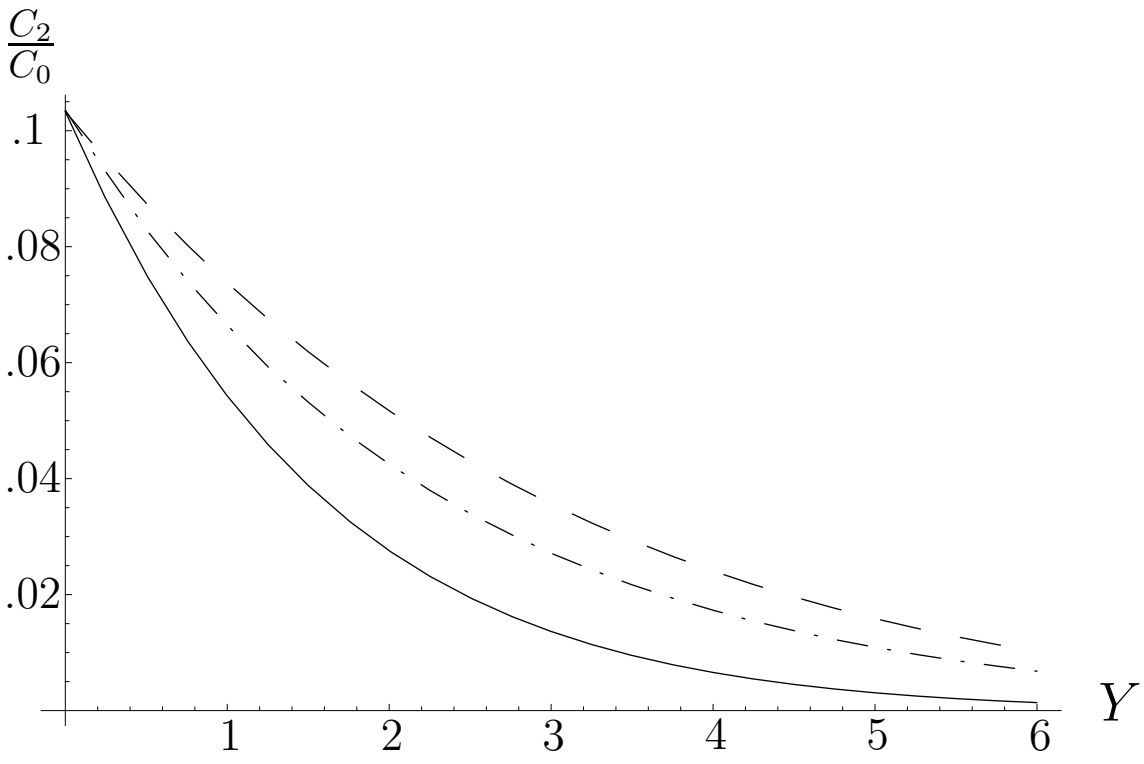

Figure 16: Forward jet production in DIS

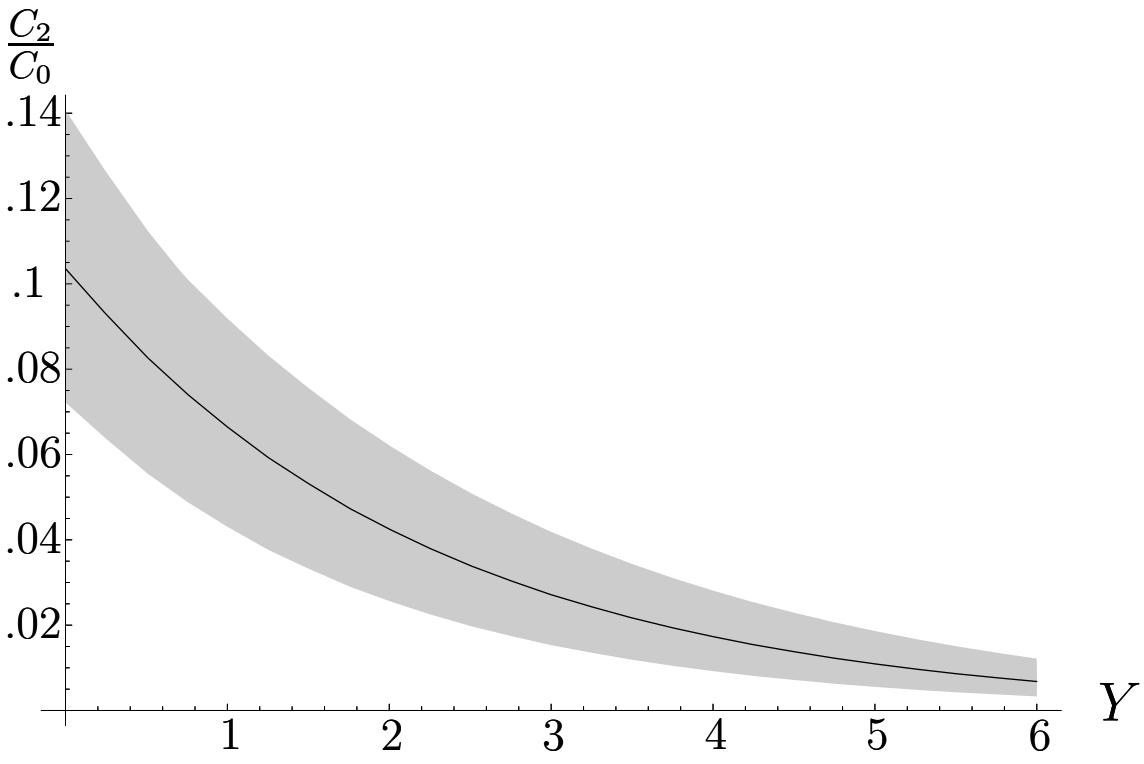

Figure 17: Forward jet production in DIS